70-21,841

TUNG, Teh-Kan, 1938-
THE STUDIES OF THE MICROWAVE SPECTRAL
LINEWIDTHS OF MOLECULES AND THE ELECTRONIC
ENERGY BAND STRUCTURES OF SOLIDS.

The University of Oklahoma, Ph.D., 1970
Physics, solid state

University Microfilms, A XEROX Company, Ann Arbor, Michigan

THE UNIVERSITY OF OKLAHOMA

GRADUATE COLLEGE

THE STUDIES OF THE MICROWAVE SPECTRAL LINEWIDTHS OF MOLECULES

AND THE ELECTRONIC ENERGY BAND STRUCTURES OF SOLIDS

A DISSERTATION

SUBMITTED TO THE GRADUATE FACULTY

in partial fulfillment of the requirements for the

degree of

DOCTOR OF PHILOSOPHY

BY
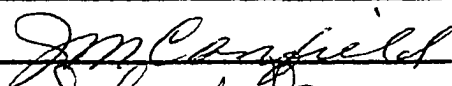
TEH-KAN TUNG

Norman, Oklahoma

1970

THE STUDIES OF THE MICROWAVE SPECTRAL LINEWIDTHS OF MOLECULES

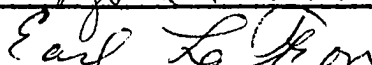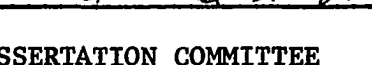AND THE ELECTRONIC ENERGY BAND STRUCTURES OF SOLIDS

APPROVED BY

S. E. Babb, Jr.

DISSERTATION COMMITTEE

ACKNOWLEDGEMENTS

The author wishes to express his deep appreciation to
Professor Chun C. Lin for suggesting the topics discussed here and
patiently directing the thesis work to its completion. He is also
indebted to Dr. Earl E. Lafon and Mr. Roy C. Chaney for many help-
ful and enlightening comments and discussions in every phase of
the work on band structures. Indeed, the success of the tight
binding method is a group effort in which the author plays but a
part.

Part of the work was done while the author was at the
University of Wisconsin at Madison and Emory University. Thanks
are due to both institutions for their support.

Last but not least, he wishes to express his gratitude to
his wife Shu-ching who in addition to her support and sacrifices
during this trying period also typed the first draft of the thesis.

TABLE OF CONTENTS

LIST OF TABLES

LIST OF ILLUSTRATIONS

PART I

LINE WIDTH OF THE ROTATIONAL SPECTRA OF

SYMMETRIC-TOP MOLECULES

CHAPTER I

INTRODUCTION

The pressure broadening of spectral lines has been of interest

for a long time. Michelson's study[1] of line broadening is perhaps the

first one in the field. In that paper, he introduced for the first time

the concept of interruption broadening due to collisions. The argument

is that a hard-sphere atom (or molecule) will undergo the process of

emitting electromagnetic wave of its natural frequency in between colli-

sions. The collision has the effect of terminating the radiations and

thus a finite wave train is formed which is our interruption broadened

spectral line after a Fourier transform is performed on it. This theory

was modified by Lorentz[2] classically. With the advent of quantum mechan-

ics, new justifications were added by Weisskopf[3] and Jablonski.[4] It was

subsequently improved by Foley[5] and Lindholm.[6]

The Fourier transform treatment gives good results in optical

region.[7] However, it fails in the microwave and infra-red regions. The

major difficulty arises from the breakdown of the adiabatic hypothesis.

In the optical region, the energy difference is much larger than the

average kinetic energy of the colliding molecules. Therefore, the

1

assumption that the probability of the collision induced transition is small is valid. This assumption is no longer valid in the microwave region since the energy difference is smaller than the average kinetic energy. Precisely for the same reason, the pressure-broadened linewidth of the rotational spectra of molecules may provide a powerful tool to study the general problem of interactions between molecules[8-10] since the linewidth will yield information about the cross sections for transfer of rotational energy and consequently the intermolecular forces.

The most successful theory for studying microwave linewidth to date was due to Anderson[11] and improved by Tsao and Curnutte.[12] This theory which is the central theme of the next chapter takes care of the diabatic effects. A number of other theoretical works on linewidth has appeared in recent years.[13-16] They vary from using different methods to arrive at the same result (Cooper, Trindle and Illinger) to slightly modified version (Murphy and Boggs). However, Anderson-Tsao-Curnutte theory is still the single most powerful tool in the study of microwave linewidth. In the subsequent chapters, we will use this theory to perform a first principle calculation of the linewidth of the rotational spectra of a number of symmetric-top molecules and compare the results with the experimental values obtained at this laboratory.

CHAPTER II

ANDERSON-TSAO-CURNUTTE THEORY

THE FORMULATION

In 1949, P. W. Anderson[11] proposed a generalized theory of collision broadening. This theory has the following basic assumptions:

1. Assumption of a classical path. It is assumed that for all collisions involved, the colliding molecules can be viewed as point dipoles traveling along a classical straight line path. For very close collision, this assumption is not valid. However, we can consider the molecules as wave packets. These wave packets are very small compared to the effective collision radius. This makes the assumption a very good one in almost all cases considered.

2. Zero collision time. The duration of the collision is very small as compared to the interval between collisions. This assumption has the effect that either the lines under consideration are degenerate or they are well-separated.

3. Binary collision. Only the collision involving a pair of molecules -- the emitter and the perturber is considered. This is seen to be valid when the pressure is sufficiently low and the temperature high.

Following Foley's approach, Anderson first wrote down the quantum mechanical expression for intensity of the spectral line due to

dipole radiation as

$$I(\omega) = \text{const} \times \omega^4 \text{ Trace}\left[\rho_0 \int_{-\infty}^{+\infty} dt\exp(i\omega t)\mu_z(t)\right.$$

$$\left. \times \int_{-\infty}^{+\infty} dt'\exp(-i\omega t')\mu_z(t')\right]. \qquad (2.1)$$

This equation has since been proved by Margenau and Bloom,[17]
where ρ_0 is the density matrix and $\mu(t)$ is the dipole matrix. Using the
time-development operator technique

$$\mu(t) = U^{-1}\mu_0 U; \quad T = U_0^{-1}U; \quad U_0 = \exp(-\tfrac{i}{\hbar}H_0 t) \quad (2.2)$$

where H_0 is the unperturbed Hamiltonian and

$$H = H_0 + H_1(t) \qquad (2.3)$$

with $H_1(t)$, the time-dependent interaction Hamiltonian. Then through
Correlation Function scheme and a rather formidable mathematical manipu-
lation, this theory gives the cross-section as

$$\sigma = \int_0^\infty 2\pi b S(b)db, \qquad (2.4)$$

where the function $S(b)$ is a weight factor governing the effectiveness
of a particular collision to interrupt a particular radiation and
impact parameter or the distance of closest approach of the molecules.
The function $S(b)$ increases as b decreases until $b = b_0$ and $S(b_0) = 1$
which means the radiation is completely interrupted.
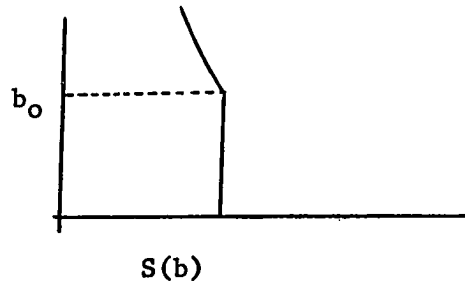
Figure 1. Relation between b and S(b).

S(b) can be expanded as

$$S(b) = S_0(b) + S_1(b) + S_2(b) + \ldots\ldots \qquad (2.5)$$

where

$$S_0(b) = 0$$

$$S_1(b) = i\left[\sum_{m_i,m_2} \frac{(j_i m_i j_2 m_2 \mid P \mid j_i m_i j_2 m_2)}{(2j_i + 1)(2j_2 + 1)}\right.$$

$$\left. - \sum_{m_f, m_2} \frac{(j_f m_f j_2 m_2 \mid P \mid j_f m_f j_2 m_2)}{(2j_f + 1)(2j_2 + 1)}\right]. \qquad (2.6)$$

It is imaginary and contributes only to the line-shift.

$$S_2(b) = S_2(b)_{outer,i} + S_2(b)_{outer,f} + S_2(b)_{middle}$$

with

$$S_2(b)_{outer,i} = \frac{1}{2}\sum_{m_i,m_2} \frac{(j_i m_i j_2 m_2 \mid P^2 \mid j_i m_i\, j_2 m_2)}{(2j_i + 1)(2j_2 + 1)} \qquad (2.7)$$

$$S_2(b)_{outer,f} = \frac{1}{2}\sum_{m_f,m_2} \frac{(j_f m_f j_2 m_2 \mid P^2 \mid j_f m_f\, j_2 m_2)}{(2j_f + 1)(2j_2 + 1)} \qquad (2.8)$$

and

$$S_2(b)_{middle} = -\sum_{\substack{m_i,m_i' \\ m_f,m_f' \\ m_2,m_2' \\ M}} \sum_{j_2'} \frac{(j_f l m_f M \mid j_i m_i)(j_f l m_f' M \mid j_i m_i')}{(2j_1 + 1)(2j_2 + 1)}$$

$$\times (j_f m_f j_2 m_2 \mid P \mid j_f m_f' j_2' m_2')$$

$$\times (j_i m_i' j_2' m_2' \mid P \mid j_i m_i j_2 m_2). \qquad (2.9)$$

Where $j_i m_i$, $j_f m_f$, $j_i' m_i'$, $j_f' m_f'$ are the quantum numbers of the initial

and final states of the emitter, $j_2 m_2$, $j_2' m_2'$ that of the perturber and

$$P = \frac{1}{\hbar}\int_{-\infty}^{+\infty} H_1'(t)dt , \qquad (2.10)$$

where H_1' is the interaction Hamiltonian with the time-dependence due to

H_1 inserted:

$$(m|H_1'|n) = (m|H_1(t)|n) \exp\left[(E_m - E_n)t/i\hbar\right]. \tag{2.11}$$

$(j_f lm_f M|j_i m_i)$ and $(j_f lm_f' M|j_2 m_2')$ are the Clebsch-Gordan

coefficients.

$S_2(b)$ is real and contributes to the linewidth. The halfwidth $\Delta\nu$

is related to the cross-section by

$$\Delta\nu = \frac{Nv\sigma}{2\pi} \tag{2.12}$$

$Nv\sigma$ gives the number of collisions per unit time. N is the number

of molecules per unit volume and v the relative molecular thermal

velocity.

Equation (2.4) gives only the collision cross section of a

emitter at a particular molecular quantum state J_1, K_1 and a

perturber at J_2, K_2. We may call it the partial cross section and

denote it by $\sigma_{J_2 K_2}$. The number of molecules in this particular

state is proportional to the statistical weight f_{JK}[18],

$$f_{JK} = \frac{S(I, K)(2J + 1)}{4I^2 + 4I + 1} \sqrt{\frac{B^2 Ch^3}{(kT)^3}}$$

$$\times \exp\left[BJ(J + 1) + (C - B)K^2\right]h/kT \tag{2.13}$$

where I is the spin quantum number. B and C are rotational con-

stants; k, the Boltzmann constant; h, Planck constant. T is the

temperature. The factor $S(I, K)$ is such that:

for K a multiple of 3, but not 0,

$$S(I, K) = 2(4I^2 + 4I + 3)f(I); \tag{2.14a}$$

for K = 0,

$$S(I, K) = (4I^2 + 4I + 3)f(I);$$ (2.14b)

for K not a multiple of 3,

$$S(I,K) = 2(4I^2 + 4I)f(I);$$

with

$$f(I) = (2I + 1)/3.$$

The cross section of a given molecule at a state J_1 and K_1 then is given by

$$\sigma_{J_1 K_1} = \sum_{J_2 K_2} f_{J_2 K_2} \sigma_{J_2 K_2}.$$

Where theoretically the summation is taken from $J_2 = 0$ to infinity with K_2- degeneracy. However, the upper limit in practice is dictated by the statistical weight such that we cut off the series when the upper levels are less populated and give insignificant contributions to the total cross section $\sigma_{J_1 K_1}$.

TSAO-CURNUTTE MODIFICATION[12]

Anderson applied his theory originally to the ammonia inversion spectral line broadening with success. It was Tsao-Curnutte modification which completes the theoretical frame work and takes into consideration the different interactions.

They expand the angular part of the interaction Hamiltonian in spherical harmonics. The general form of the matrix element P is then of the form

$$(j_1 m_1 j_2 m_2 |P| j_1 'm_1' j_2 'm_2')$$

$$= \sum_{\substack{k_1 k_2 \\ \lambda_1 \lambda_2}} a(\lambda k j)(j_1 m_1 j_2 m_2 |Y_{\lambda_1}^{k_1}(1) Y_{\lambda_2}^{k_2}(2)| j_1 'm_1' j_2 'm_2').$$

(2.14)

Where $Y_\lambda^k(\phi\theta)$ are the apherical harmonics. For symmetric-top molecules the matrix elements are

$$(j'K'm'|Y_\lambda^k(\phi\theta)|jKm) = \left[\frac{(2j+1)(2K+1)}{4\pi(2j'+1)}\right]^{\frac{1}{2}}$$

$$\times(jkK0|j'K')(jkm\lambda|j'm'). \qquad (2.15)$$

The quantum numbers are related as

$$j+k = j', \quad K+0 = K', \quad m+\lambda = m'.$$

The modified expressions of $S_2(b)$ are:

$$S_2(b)_{outer,i} = \frac{1}{32\pi^2}\sum_{\substack{j_i'j_2'\\k_1\,k_2\\\lambda_1\,\lambda_2}}' (j_ik_1K_i0|j_i'K_i)^2$$

$$\times(j_2k_2K_20|j_2'K_2)^2|a(\lambda kj)|^2 \qquad (2.16a)$$

$$S_2(b)_{outer,f} = \frac{1}{32\pi^2}\sum_{\substack{j_f'j_2'\\k_1\,k_2\\\lambda_1\,\lambda_2}}' (j_fk_1K_f0|j_f'K_f)^2$$

$$\times(j_2k_2K_20|j_2'K_2)^2|a(\lambda kj)|^2 \qquad (2.16b)$$

and

$$S_2(b)_{middle} = (-1)^{j_i+j_f}\frac{\sqrt{(2j_i+1)(2j_f+1)}}{16\pi^2}$$

$$\times\sum_{k_1k_2j_2'}\sum_{\lambda_1\lambda_2}(-1)^{k_1+\lambda_1+\lambda_2}(j_ik_1K_i0|j_iK_i)$$

$$\times(j_fk_fK_f0|j_fK_f)(j_2k_2K_20|j_2'K_2)^2$$

$$\times W(j_ij_fj_ij_f,1k_1)a(k_1k_2\lambda_1\lambda_2j)$$

$$\times a'(k_1k_2-\lambda_1-\lambda_2j') \qquad (2.17)$$

where W is the Racah's coefficient.

DIPOLE-DIPOLE INTERACTION

The classical dipole-dipole interaction between two molecules is given by the expression

$$\vec{P_1} \cdot \vec{P_2} - 3(\vec{P_1} \cdot \vec{R_o})(\vec{P_2} \cdot \vec{R_o})/R^3 \ ,$$

where $\vec{P_1}$, $\vec{P_2}$ are the dipole moments of the molecules, R is the distance between the molecules and $\vec{R_o}$ is the unit vector along R. For linear or symmetric-top molecules, the dipole moment can be specified by its magnitude and the direction of the symmetry axis.

The interaction Hamiltonian is then

$$(m|p|n) = \frac{P_1 P_2}{\hbar} (G_1 F_1 + G_2 F_2 + G_3 F_3)_{mn}, \qquad (2.18)$$

where

$$F_1 = \sin\theta_1 \cos\phi_1 \sin\theta_2 \cos\phi_2 - 2\sin\theta_1 \sin\phi_1 \sin\theta_2 \sin\phi_2 + \cos\theta_1 \cos\theta_2$$

$$F_2 = 3\sin\theta_1 \sin\phi_1 \cos\theta_2 + 3\cos\theta_1 \sin\theta_2 \sin\phi_2 \qquad (2.19)$$

$$F_3 = 3\sin\theta_1 \sin\phi_1 \sin\theta_2 \sin\phi_2 - 3\cos\theta_1 \cos\theta_2$$

$$G_1 = \int_{-\infty}^{+\infty} \frac{\exp(i\omega mnt)}{R^3} \, dt$$

$$G_2 = \int_{-\infty}^{+\infty} \frac{\exp(i\omega mnt)\sin\psi\cos\psi}{R^3} \, dt \qquad (2.20)$$

$$G_3 = \int_{-\infty}^{+\infty} \frac{\exp(i\omega mnt)\cos^2\psi}{R^3} \, dt \ ,$$

where (ϕ_1, θ_1) and (ϕ_2, θ_2) are the direction of the dipole P_1 and P_2 respectively. The quantities R and ψ depend on time.
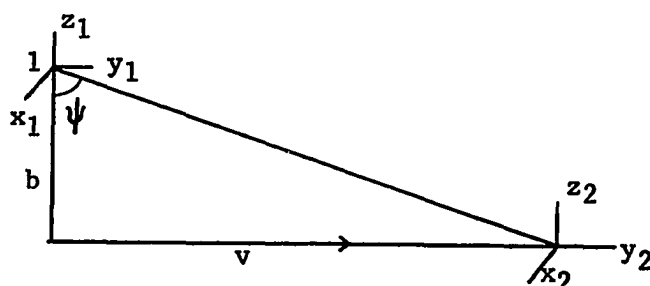
Figure 2. Diagram of the coordinates

If v is the velocity of the collision, then

$$R = \sqrt{(b^2 + v^2 t^2)} \tag{2.21}$$

$$\sin \psi = \frac{vt}{R} \qquad \cos \psi = \frac{b}{R} .$$

In Anderson's original application of the theory to ammonia inversion spectral lines, he ignored the G's entirely as he took into consideration only the first order Stark effect and rotational resonance. These approximations are valid since the ammonia molecule is a rather unique case in that the rotational energy levels occur in closely spaced pairs of about 1 cm^{-1} due to inversion and that levels of different rotational quantum numbers J are generally separated by over 20 cm^{-1}. Because of this pattern of energy levels, one needs to consider energy transfer only between the two inversion levels of a given rotational state during the process of collision interruption of radiation. The collision induced transitions of type $J \rightarrow J'$ ($J' \neq J$) are expected to have much smaller cross-sections on account of the large energy differences and are neglected aside from the case of rotational resonance. Furthermore, for the purpose of computing collision induced transition probabilities between the two inversion doublets, the energy spacing between these pairs are set to zero.

For the symmetric-top molecules, the rotational constants

which govern the frequencies of the J transition are less than 14

kMc/sec, hence the approximations are no longer valid. The integrals

of G's must be evaluated. It was shown[12] that:

$$G_1 = \frac{1}{vb^2} \, 2\,|k|\, K_1(\,|k|\,)$$

$$G_2 = \frac{1}{vb^2}' \, i \, \frac{2}{3} \, \frac{k}{|k|} \, k^2 K_1(\,|k|\,) \qquad (2.22)$$

$$G_3 = \frac{1}{vb^2} \, \frac{2}{3} \, k^2 K_2(\,|k|\,)$$

where

$$k = \frac{b}{v}\omega_{mn} \, , \qquad (2.23)$$

and K, the Bessel function of the second kind.

We can also write F's in terms of the spherical harmonics:

$$F_1 = 2\pi[Y_1^{\ 1}(1)Y_1^{\ 1}(2) + Y_{-1}^{\ 1}(1)Y_{-1}^{\ 1}(2)]$$

$$+ \frac{2\pi}{3}[Y_1^{\ 1})1)Y_{-1}^{\ 1}(2) + Y_{-1}^{\ 1}(1)Y_1^{\ 1}(2)]$$

$$+ \frac{4\pi}{3}Y_0^{\ 1}(1)Y_1^{\ 1}(2) \, ,$$

$$F_2 = i \cdot 2 \, \sqrt{2}\pi[Y_1^{\ 1}(1)Y_0^{\ 1}(2) + Y_{-1}^{\ 1}(1)Y_0^{\ 1}(2) + Y_0^{\ 1}(1)Y_1^{\ 1}(2)$$

$$+ Y_0^{\ 1}(1)Y_{-1}^{\ 1}(2)] \, ,$$

$$F = -2\pi[Y_1^{\ 1}(1)Y_1^{\ 1}(2) + Y_{-1}^{\ 1}(1)Y_{-1}^{\ 1}(2) + Y_{-1}^{\ 1}(1)Y_1^{\ 1}(2)$$

$$+ Y_1^{\ 1}(1)Y_{-1}^{\ 1}(2)] - 4\pi Y_0^{\ 1}(1)Y_0^{\ 1}(2) \, . \qquad (2.24)$$

Substituting the expressions of F's and G's into (2.16a),

(2.16b), and (2.17), we obtain

$$S_2(b)_{0,1} = \frac{4}{9}\left(\frac{P_1P_2}{\hbar v}\right)^2 \frac{1}{b^4} \sum_{j_1'j_2} (j_1 1 K_i 0 | j_i' K_i)^2$$

$$\times \, (j_2 1 K_2 0 | j_2' K_2)^2 \, f_1(k) \, , \qquad (2.25)$$

where

$$f_1(k) = \frac{1}{4} k^2 [K_2{}^2(k) + 4K_1{}^2(k) + 3K_0{}^2(k)] \qquad (2.26)$$

with similar expression for $S_2(b)_{o,f}$. The function $S_2(b)_m$ is
is expressed as

$$S_2(b)_m = (-1)^{j_i + j_f + 1} \cdot \frac{8}{9} \left(\frac{p_1 p_2}{\hbar v}\right)^2 \frac{1}{b^4} \sqrt{(2j_i + 1)(2j_f + 1)}$$

$$\times (j_i 1 K_i 0 | j_i k_i) \times (j_f 1 K_f 0 | j_f K_f)$$

$$\times W(j_i j_f j_i j_f, 11) \sum_{j_2{}'} (j_2 1 K_2 0 | j_2{}' K_2)^2 \cdot f_1(k) \quad . \quad (2.27)$$

Once the $S_2(b)$ is known, we adopt the "approximation #2" of the interpolation process of Anderson. Let b_0 be the value of b at which

$$S_2(b_0) = 1 \qquad (2.28)$$

then

$$\sigma_{j_2 k_2} = \pi b_0{}^2 + \int_{b_0}^{\infty} (2\pi b) db [S_2(b)_{o,i} + S_2(b)_{o,f}$$

$$+ S_2(b)_m]. \qquad (2.29)$$

The integrand is evaluated to yield

$$\frac{1}{2} b_0{}^2 [K_3 K_1 + 4K_0 K_2 - K_2{}^2 - K_1{}^2 - 3K_0{}^2]_{k=k_0} \qquad (2.30)$$

COMPUTABLE FORM

As previously pointed out, in evaluating the line width of the symmetric-top molecules, the Anderson's approximations applied to ammonia inversion are no longer valid. We must now include all the interaction between the emitter and the perturber during the collision. There are the following transitions which occur in the collision process:

$$\Delta J_1 = \Delta J_2 = 0 \tag{2.31}$$

$$\Delta J_1 = \pm 1, \Delta J_2 = 0 \tag{2.32}$$

$$\Delta J_1 = \pm 1, \Delta J_2 = \mp 1 \tag{2.33}$$

$$\Delta J_1 = 0, \pm 1, \Delta J_2 = \pm 1. \tag{2.34}$$

For the $J_1 = 0 \rightarrow 1$ transition, Birnbaum found that processes (2.31) and (2.32) occur with much higher probability than the others.[19]

By neglecting the transitions (2.33) and (2.34) and setting $E(J_1 = 1) - E(J_1 = 0) \simeq 0$, Birnbaum obtained a rather simple expression for the linewidth:

$$\Delta \nu_{J_1 K_1} = \left(\frac{8}{9}\right)\frac{\frac{1}{2}NP_1P_1}{\hbar}\left[1 - \frac{K_1^2}{(J_1+1)^2}\right]^{\frac{1}{2}} x \left\langle \frac{K_2}{[J_2(J_2+1)]^{\frac{1}{2}}} \right\rangle . \tag{2.35}$$

Where the expression $\langle \rangle$ is the Boltzmann average of the quantity. However, our calculations in the next chapter will show that for the higher transitions ($J_1 = 1,2$ or above) this approximation is invalid.

Including all the processes cited above, and the proper values for both Clebsch-Gordan coefficients[20] and Racah's coefficients,[21] we obtain the following equation, the detailed evaluation will be given in Appendix A.

$$S_2(b) = \frac{4}{9}\left(\frac{P_1P_2}{\hbar v}\right)^2 \frac{1}{b^4}\left\{\frac{K_2^2}{J_2(J_2+1)}\left(\frac{K_1^2}{J(J_1+1)} + \frac{K_1^2}{(J_1+1)(J_1+2)}\right.\right.$$

$$\left.- \frac{2K_1^2}{(J_1+1)^2}\right) + \frac{J_2^2 - K_2^2}{J_2(2J+1)}\left(\frac{(J_1+1)^2 - K_1^2}{(2J_1+1)(J_1+1)}\right.$$

$$\left. f_1(x(J_1-J_2+1)) + \frac{(J_1+2)^2 - K_1^2}{(2J_1+3)(J_1+2)} f_1(x(J_1-J_2+2))\right)$$

$$+ \frac{(J_2-1)^2 - K_2^2}{(2J_2+1)(J_2+1)} \left(\frac{J_1^2-K_1^2}{J_1(2J_1+1)} \, f_1(x(J_2-J_1+1)) \right.$$

$$+ \frac{(J_1+1)^2-K_1^2}{(J_1+1)(2J_1+3)} \, f_1(x(J_2-J_1))) $$

$$+ \frac{K_2^2}{J_2(J_2+1)} \left(\frac{(J_1+1)^2-K_1^2}{(2J_1+1)(J_1+1)} \, f_1(x(J_1+1)) \right.$$

$$+ \frac{(J_1+2)^2-K_1^2}{(2J_1+3)(J_1+2)} \, f_1(x(J_1+2))$$

$$+ \frac{J_1^2-K_1^2}{J_1(2J_1+1)} \, f_1(x(J_1))$$

$$+ \frac{(J_1+1)^2-K_1^2}{(J_1+1)(2J_1+3)} \, f_1(x(J_1+1)))$$

$$+ \frac{(J_2+1)^2-K_2^2}{(2J_2+1)(J_2+1)} \left(\frac{K_1^2}{J_1(J_1+1)} + \frac{K_1^2}{(J_1+1)(J_1+2)} \right.$$

$$- \frac{2K_1^2}{(J_1+1)^2} \, f_1(x(J_2+1))$$

$$+ \frac{J_2^2-K_2^2}{J_2(2J_2+1)} \left(\frac{K_1^2}{J_1(J_1+1)} + \frac{K_1^2}{(J_1+1)(J_1+2)} - \frac{2K_1^2}{(J_1+1)^2} \, f_1(xJ_2) \right.$$

$$+ \frac{(J_2+1)^2-K_2^2}{(2J_2+1)(J_2+1)} \left(\frac{(J_1+1)^2-K_1^2}{(2J_1+1)(J_1+1)} \, f_1(x(J_1+J_2+2)) \right.$$

$$+ \frac{(J_1+2)^2-K_1^2}{(2J_1+3)(J_1+2)} \, f_1(x(J_1+J_2+3)))$$

$$+ \frac{(J_2-K_2)(J_2+K_2)}{J_2(2J_2+1)} \quad (\frac{J_1^2-K_1^2}{J_1(2J_1+1)} f_1(x(J_1+J_2))$$

$$+ \frac{(J_1+1)^2-K_1^2}{(J_1+1)(2J_1+3)} f_1(x(J_1+J_2+1)))\}$$

$$(2.36)$$

where $x = 4\pi bB/v$.

CHAPTER III

COMPARISON BETWEEN THEORY AND EXPERIMENT

NUMERICAL CALCULATION

Once the analytical form of $S_2(b)$ is known, we proceed to find b_o such that $S_2(b_o) = 1$. The method used in this study is the standard Newton's method.[22] In the present work, self-broadening of seven different symmetric-top molecules are studied. They are: CH_3Br^{79}, CH_3Br^{81}, CH_3I, CH_3Cl^{35}, CH_3Cl^{37}, CH_3CN and CH_3CH. Only dipole-dipole interaction is considered since this is the dominating term for collision.

The calculation was carried out on a CDC3400 computer. Except some physical constants such as mass number, Planck's constant, etc., the only input are two rotational constants B and C and the dipole moment. A list of these values and their sources are given in Table I.

The choice of the velocity, which is very crucial to the linewidth, is that of the relative velocity average over the Boltzmann distribution. This choice is justified since at sufficient low pressure and room temperature the gases under consideration do obey the Maxwell-Boltzmann distribution. Thus the velocity of the gas is:

$$\bar{v} = \sqrt{\frac{8KT}{\pi m}} \qquad \cdot \qquad (3.1)$$

For the relative velocity of two colliding molecules, the m is re-placed by the reduced mass μ[23] and

$$\bar{v}_{re} = \sqrt{\frac{8KT}{\pi\mu}} \qquad (3.2)$$

The calculated values are listed in Table II. They are compared with the experimental values obtained at this laboratory.[25] In the calculation of the linewidths, we have neglected the hyper-fine splitting, namely, the width of the $J \rightarrow J+1$ rather than J, $F \rightarrow J+1$, F' transitions were calculated.

For CH_3Cl, and CH_3Br the broadening effect of different isotopic species, e.g., $CH_3Cl^{35} - CH_3Cl^{35}$ and $CH_3Cl^{35} - CH_3Cl^{37}$, etc., must be computed separately. Since the energy differences in (2.31) - (2.34) cannot be neglected in computing $S_2(b)$, one can no longer expect the relative linewidths of a given molecule to be independent of the method of interpolation. For this reason the experimental date will be compared with the theoretical values of the absolute linewidths rather than the relative widths.

Except for the case of the CH_3CCH molecule, the theoretical widths are generally larger than the experimental ones. This is most noticeable in both isotopes of CH_3Cl where one observes a dif-ference of about 30%. Equally larger percentage differences are found for the low-J lines of CH_3Br^{79} and CH_3Br^{81}, but the agreement becomes better at higher J. The CH_3I lines show variations from 2% to 30% between theory and experiment. The same is true also for CH_3CCH except that the measured widths are consistently larger than the theoretical values in this case, because this molecule has a

TABLE I

THE CONSTANTS FOR THE GASES

Gas	B in Mc/s	C in Mc/s	Dipole-moment in Debye
CH_3Br^{79}	9568.19*	$148 \times 10^{3\#}$	1.797*
CH_3Br^{81}	9531.84*	$148 \times 10^{3\#}$	1.797*
CH_3Cl^{35}	13292.84*	$150 \times 10^{3+}$	1.869*
CH_3Cl^{37}	13088.137*	$150 \times 10^{3+}$	1.869*
CH_3CH	8545.85*	$150 \times 10^{3+}$	0.75*
CH_3I^{127}	7501.31*	$150 \times 10^{3+}$	1.65*
CH_3CN	9198.83*	$150 \times 10^{3+}$	3.92*

* reference 14.

+ reference 24.

calculated by the author by standard method.

TABLE II

LINEWIDTH PARAMETERS (Mc/s — torr)

OF SYMMETRIC-TOP MOLECULES.

Gas	ΔJ	K	ΔF	$(\Delta \nu_p)_{Obs}$	$(\Delta \nu_p)_{Calc}$
CH_3Cl^{35}	0 — 1	0	$\frac{3}{2} - \frac{5}{2}$	19.5	25.30
	1 — 2	0	$\frac{5}{2} - \frac{7}{2}$	17.6	23.72
		1	$\frac{5}{2} - \frac{7}{2}$	15.6	21.00
CH_3Cl^{37}	0 — 1	0	$\frac{3}{2} - \frac{5}{2}$	20.2	25.22
	1 — 2	0	$\frac{5}{2} - \frac{7}{2}$	17.9	23.60
	2 — 3	0	$\frac{7}{2} - \frac{7}{2}$	12.8	21.81
CH_3Br^{79}	0 — 1	0	$\frac{3}{2} - \frac{5}{2}$	15.7	19.87
	1 — 2	0	$\frac{1}{2} - \frac{3}{2}$	13.6	18.37
		1	$\frac{5}{2} - \frac{7}{2}$	12.3	16.22
	2 — 3	0	$\frac{7}{2} - \frac{7}{2}$	12.8	16.72
		1	$\frac{7}{2} - \frac{9}{2}$	11.8	16.02
		2	$\frac{1}{2} - \frac{3}{2}$	11.9	13.46

TABLE II (Continued)

Gas	Δ J	K	Δ F	$(\Delta\nu_p)_{Obs}$	$(\Delta\nu_p)_{Calc}$
CH_3Br^{79}	3 — 4	0	$\frac{5}{2} - \frac{7}{2}$	12.8	15.50
		1	$\frac{7}{2} - \frac{9}{2}$	13.8	15.20
		2	$\frac{9}{2} - \frac{11}{2}$	12.6	14.11
		3	$\frac{7}{2} - \frac{9}{2}$	12.0[a]	11.85
CH_3Br^{81}	0 — 1	0	$\frac{3}{2} - \frac{5}{2}$	15.2	19.84
	1 — 2	0	$\frac{1}{2} - \frac{3}{2}$	13.3	18.32
		1	$\frac{5}{2} - \frac{7}{2}$	12.9	16.17
	2 — 3	0	$\frac{5}{2} - \frac{5}{2}$	12.9	16.66
		2	$\frac{1}{2} - \frac{3}{2}$	12.9[a]	13.41
	3 — 4	1	$\frac{7}{2} - \frac{9}{2}$	13.2	15.12
		2	$\frac{9}{2} - \frac{11}{2}$	12.9	14.08
		3	$\frac{3}{2} - \frac{5}{2}$	12.7[a]	11.81
CH_3I	0 — 1	0	$\frac{5}{2} - \frac{7}{2}$	13.3	15.00
	1 — 2	0	$\frac{7}{2} - \frac{9}{2}$	10.8	13.97
		1	$\frac{7}{2} - \frac{9}{2}$	9.6	12.33

TABLE II (Continued)

Gas	ΔJ	K	ΔF	$(\Delta\nu_P)_{Obs}$	$(\Delta\nu_P)_{Calc}$
CH_3I	2 — 3	0	$\frac{9}{2} - \frac{11}{2}$	9.5^a	12.79
		2	$\frac{9}{2} - \frac{9}{2}$	9.5	10.26
	3 — 4	0	$\frac{3}{2} - \frac{5}{2}$	9.5	11.87
		1	$\frac{11}{2} - \frac{11}{2}$	9.5	11.62
		2	$\frac{11}{2} - \frac{13}{2}$	9.6	10.81
		3	$\frac{11}{2} - \frac{13}{2}$	8.8	9 03
	4 — 5	0	$\frac{11}{2} - \frac{13}{2}$	9 8	11.37
		1	$\frac{13}{2} - \frac{15}{2}$	9.7	11.23
		2	$\frac{13}{2} - \frac{15}{2}$	9.9	10.79
		3	$\frac{13}{2} - \frac{15}{2}$	9.7	9.94
CH_3CN	0 — 1	0	1 — 2	94.2	91.67
C_3H_4	0 — 1	0		8.7	7.04
	1 — 2	0		8.0^b	7.10
		1		8.2^b	6.45
	2 — 3	0		7.3	7.18
		1		8.5	6.90
		2		8.4	5.88

TABLE II (Continued)

Gas	ΔJ	K	ΔF	$(\Delta\nu_p)_{Obs}$	$(\Delta\nu_p)_{Calc}$
C_3H_4	3 ⇌ 4	0		8.5	7.26
		1		8.6	7.11
		2		7.9	6.58
		3		7.9	5.46

[a] Poor accuracy because of standing waves.

[b] The K = 0 and K = 1 components of the J = 1 2 transition of C_3H_4 are separated by only 0.7 Mc/sec. The linewidth data for these two lines are less accurate because of the neighbor-line interference.

rather small dipole moment (0.75D) and because the theoretical widths

were calculated using only dipole-dipole force. Inclusion of the

quadrupole interaction has been attempted but the result is not

impressive. In view of the disagreement of the same magnitude

existing in other molecules, the quadrupole contribution to line-

widths of CH_3CCH is very difficult to pinpoint. The theoretical

width comes very close to experimental value for the $0 \to 1$ line of

CH_3CN. The unusually larger linewidth is due to the large dipole

moment (3.92D).

The theoretical linewidths decrease with increasing J for

each J, K $\to$J+1, K series (fixed K), and decrease with increasing K

in the sequence J, K $\to$J+1, K for a given J. This trend is not

always clear in the experimental data; when it is evident, the rate

of decrease of linewidths with respect to the quantum numbers is

smaller than predicted by theory. If we normalize one theoretical

width to its corresponding experimental value for each molecule,

the relative theoretical linewidths so obtained naturally show better

agreement with experiment. This is especially true of CH_3Cl, but the

degree of improvement for the other molecules is not particularly

impressive.

AMMONIA SELF-BROADENING

In order to find out the extent of the validity of the approx-

imations employed in the calculation of the linewidth of ammonia

inversion spectral lines, we also calculated the line width for

ammonia self-broadening using the exact expression of (2.36). The

results are tabulated in Table III where $(\Delta\nu)_{obs}$ and $(\Delta\nu)_1$ are taken from reference 26. $(\Delta\nu)_2$ is the exact calculation of the absolute linewidth. It is obvious that if $(\Delta\nu)_2$ is normalized, a fairly good agreement between $(\Delta\nu)_1$ and $(\Delta\nu)_2$ is yield which indicates that the approximation is a good one.

TABLE III

LINEWIDTH PARAMETERS (Mc/s-torr)

OF SELF-BROADENING OF NH_3

Lines	$(\Delta\nu)_{obs}$	$(\Delta\nu)_1$	$(\Delta\nu)_2$	Lines	$(\Delta\nu)_{obs}$	$(\Delta\nu)_1$	$(\Delta\nu)_2$
(2,2)	22.3	22.6	29.7	(4,3)	22.1	20.1	26.1
(3,3)	24.0	23.9	31.4	(4,2)	16.1	14.5	19.7
(4,4)	24.4	(24.4)	32.2	(4,1)	13.4	10.3	13.4
(5,5)	24.6	24.7	32.6	(6,5)	22.0	22.0	28.5
(6,6)	24.0	24.9	32.8	(6,4)	19.6	18.4	24.0
(7,7)	24.6	25.0	33.0	(6,3)	16.6	14.9	19.5
(8,8)	24.7	25.1	33.2	(6,2)	13.8	11.5	14.9
(9,9)	24.6	25.2	33.4	(8,7)	21.9	22.5	29.5
(10,10)	23.8	25.3	33.6	(8,6)	19.8	19.5	25.7
(3,2)	17.6	17.6	23.0	(8,5)	17.5	16.7	21.9
(3,1)	12.8	11.0	14.4	(10,9)	21.2	23.0	30.2

PART II

APPLICATION OF THE GAUSSIAN-TYPE ORBITALS FOR

CALCULATING ENERGY BAND STRUCTURES OF

SOLIDS BY THE METHOD OF TIGHT BINDING

CHAPTER IV

INTRODUCTION

The electronic energy band structure of crystalline materials

has been of great scientific interest for many years and has been

studied very extensively both experimentally and theoretically.

There are a number of diversive methods employed by various authors[27]

in solving this problem. They range from such ab initio calculation

of self-consistant-field method of Herman[28] to empirically adjusted

pseudo-potential approach of Cohen.[29] Among them one of the oldest

and perhaps the more physical ones is the tight-binding method of

Bloch.[30]

Bloch's method is basically an one-electron model. It con-

sists of making the linear combination of atomic orbitals located at

various atomic sites to form the so-called "Bloch sum" and use the

Bloch sum as basis functions to solve the eigenvalue problem. Before

the advent of high speed computers, the main difficulty of applying

this method lay in the fact that, in order to evaluate the necessary

matrix elements, a large number of multi-center integrals had to be

evaluated, which was an almost impossible task as late as 1954.[31]

The first breakthrough in this respect is due to Lafon and Lin.[32]
In their calculation of the band structure of lithum, they success-
fully evaluated all the necessary integrals involved without
resorting to any adjustable parameter scheme for tight-binding
calculation for the first time.

Atomic orbitals generally assume the form of the linear
combinations of exponential functions known as Slater orbitals. The
Slater orbitals are the well-known exponential functions of the form
$\exp(-\alpha r)$ for s-state, $x\exp(-\alpha r)$ for p-state, etc. For Gaussians, we
shall use $\exp(-\alpha r^2)$ or $G^s(\alpha, \vec{r})$ to represent an s-state and
$x\exp(-\alpha r^2)$ or $G^{Px}(\alpha, \vec{r})$ for a p-state Gaussian; and $G(\alpha, \vec{r})$ for
either an s- or a p-state Gaussian. To evaluate the integrals aris-
ing from two Slater orbitals situated at two different sites is the
major difficulty encountered in the molecular calculations. On the
other hand, it is known that the Gaussian function has a certain
property which is very desirable in evaluating multi-center integrals,
namely, the product of the two Gaussians having different centers A
and B is itself a Gaussian with a center C somewhere on the line set-
ment joining the two centers, i.e.,

$$G_i(\alpha_i, \vec{r}_A)G_j(\alpha_j, \vec{r}_B) = KG_k(\alpha_k, \vec{r}_C), \tag{4.1}$$

where K is a constant such that

$$K = \exp(-\frac{\alpha_i \alpha_j}{\alpha_i + \alpha_j} \overline{AB}^2), \tag{4.2}$$

and
$$\alpha_k = \alpha_i + \alpha_j; \tag{4.3}$$

$$C_x = \frac{\alpha_i A_x + \alpha_j B_x}{\alpha_i + \alpha_j} \; ; \qquad C_y = \frac{\alpha_i A_y + \alpha_j B_y}{\alpha_i + \alpha_j} \; ;$$

$$C_z = \frac{\alpha_i A_z + \alpha_j B_z}{\alpha_i + \alpha_j} \; . \qquad\qquad (4.4)$$

Therefore, a Slater orbital of the form $\exp(-\alpha r)$ can be transformed

through an integral transformation of the form

$$\exp(-\alpha r) = (\frac{\alpha}{2/\pi}) \int_0^\infty s^{\frac{3}{2}} \exp(-\frac{\alpha^2}{4s}) \exp(sr^2) ds. \qquad (4.5)$$

A multi-center integral can thus be reduced to a single-center

integral. The integration over the parameter s is usually handled

by numerical integration. In their calculations of lithum and

diamond[34] band structure, a Gaussian quadrature was employed. They

proved that the tight-binding method is not only good for the co-

valent crystal such as diamond but is also very effective for metal

like lithum where the valence electron is not tightly bound.

The success of Lafon and Lin points out the attractive features of

the tight-binding method applied to solids. In these authors'

opinion, it should be properly called LCAO (linear combination of

atomic orbitals) method.

As early as 1950, Boys[35] proposed that the atomic orbitals be

expressed as the linear combination of Gaussian functions. Subse-

quently a number of investigations were carried out to apply the

Gaussian orbitals to the molecular calculations.[36] The differences

between using Gaussian-type-orbitals (GTO) and Slater-type-orbitals

(STO) as atomic functions are:

1. Since the Gaussians fall off more rapidly than the Slater orbitals, it requires more Gaussians with a large range of magnitude of Gaussian exponential parameters to represent a wave function which could be represented by a smaller number of moderate size Slater orbitals. Besides, even with a large number of Gaussians, the GTO still fail to represent the tail part of the wave functions satisfactorily due to the sharp-decay nature of the Gaussian functions.

2. In carrying out the multi-center integrals, the integral transformation (4.5) is no longer necessary. The computational labor involved is greatly reduced.

The present work applies the Gaussian orbitals to the energy band calculation. The purpose is two-fold:

1. To investigate the effect which the longer range wave functions have on the energy band structure, Lafon and Lin have shown that the major cause contributed to the failure of the previous tight-binding calculation was the so-called "nearest neighbor approximation" which only takes care of the interaction between the nearest neighboring atoms or the next-nearest neighboring atoms in the crystal and ignores the ones which were separated at larger distance in order to reduce the number of the troublesome multicenter integrals. On the other hand, it will give us additional insight into the problem if we could find out how important the tail part of the wave function is as far as energy band calculation is concerned. A replacement of STO by GTO amounts to a "cut-off" procedure for the wave functions.

2. A reduction of computer time will make the tight-binding

method a practical and feasible one. It is estimated that for the band structure of lithum,[37] the GTO approach requires two minutes on the Univac 1108 at the University of Wisconsin Computer Center. The amount required for diamond is about five minutes. The STO requires hours on the CDC 3400. The results of these two different basis functions give excellent agreement to each other. Hence we speed up the computational time by a fairly large factor without any significant loss of accuracy.

It is believed that the Gaussian-type-orbitals will be a feasible tool to study the one-electron model of the solids. It is likely that electronic energy band structure will be but one of the many calculations GTO is capable of yielding useful information.

CHAPTER V

CRYSTAL LATTICE AND CRYSTAL POTENTIAL

CRYSTAL LATTICE

The space lattice of diamond is face-centered cubic with a
basis of two atoms at $(0, 0, 0)$ and $(\frac{1}{4}, \frac{1}{4}, \frac{1}{4})$ associated with each
lattice point. The crystal can be considered as composed of two
interpenetrating face-centered cubic lattices displaced by a
quarter of a lattice constant along the body diagonal.

For the face-centered cubic lattice, the periodicity of the
crystal lattice can be represented by a set of vector $\vec{R}_n$ defined
such that a translation by any $\vec{R}_n$ will produce the potential at the
starting point. $\vec{R}_n$ is represented by the expression

$$\vec{R}_n = n_1\vec{a}_1 + n_2\vec{a}_2 + n_3\vec{a}_3 \quad , \tag{5.1}$$

where the n's are the shortest possible independent periodic trans-
lations in the lattice. For fcc lattice:

$$\vec{a}_1 = \frac{a_o}{2}(1,1,0);$$

$$\vec{a}_2 = \frac{a_o}{2}(1,0,1);$$

$$\vec{a}_3 = \frac{a_o}{2}(0,1,1), \tag{5.2}$$

where a_o is the lattice constant.

31
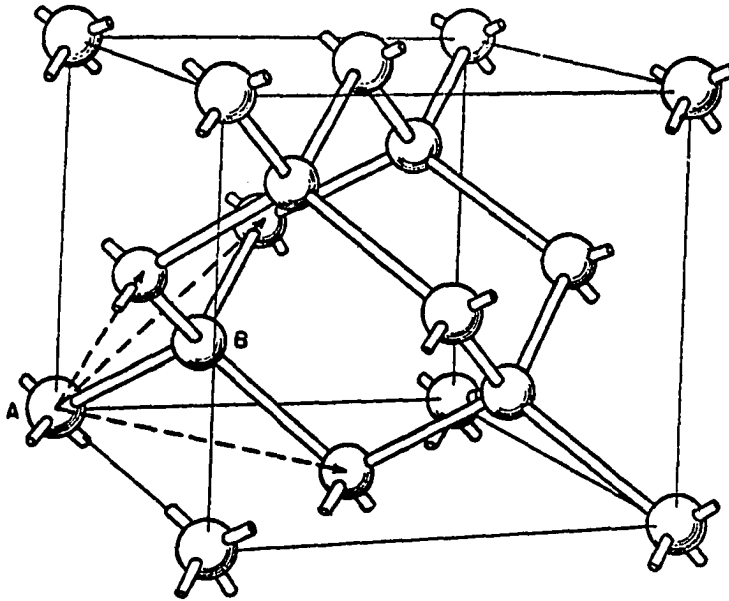
Fig. 3   Crystal Structure of Diamond
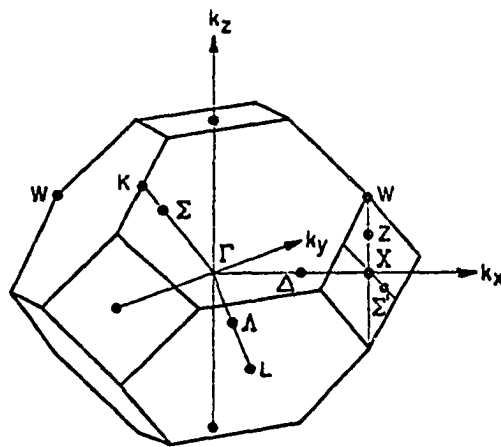
Fig. 4   The Reciprocal Lattice of the fcc Lattice

Now we define another set of vectors which spans the space of the "reciprocal lattice." The significance of this space will be evident in the next chapter. We define another set of vector $\vec{K_m}$ such that

$$\vec{K_m} \cdot \vec{R_n} = 2\pi l_{mn} , \qquad (5.3)$$

where l_{mn} are the integers. The set of vector $\vec{K_m}$ form the reciprocal lattice. In terms of the shortest possible independent periodic translations in the reciprocal lattice,

$$\vec{K_m} = m_1\vec{b_1} + m_2\vec{b_2} + m_3\vec{b_3} . \qquad (5.4)$$

The reciprocal lattice for fcc lattice is itself a body-centered cubic and

$$\vec{b_1} = \frac{2\pi}{a_o} (1, 1, -1);$$

$$\vec{b_2} = \frac{2\pi}{a_o} (1, -1, 1) ;$$

$$\vec{b_3} = \frac{2\pi}{a_o} (-1, 1, 1) . \qquad (5.5)$$

CRYSTAL POTENTIAL

The Schroedinger equation for an electron moving in a perfectly periodic crystal lattice is

$$[-\frac{1}{2}\nabla^2 + V(\vec{r})] \psi (r) = E(\vec{r}), \qquad (5.6)$$

where atomic units are used.[38]

  unit of mass = the rest-mass of the electron

  unit of charge = $|e|$, the magnitude of the charge

      on the electron

  unit of length = the radius of the first Bohr orbit

      of the hydrogen atom

unit of energy = twice the ionization energy of the

normal state of hydrogen atom.

$V(\vec{r})$ is the crystal potential and according to Bloch's

theorem, the solution must have the form

$$\psi_{\vec{k}}(\vec{r}) = \exp(i\vec{k} \cdot \vec{r}) \, U_{\vec{k}}(\vec{r}), \qquad (5.7)$$

where $\vec{k}$ is the crystal momentum. The choice of crystal potential

is such that it will represent a first approximation of the true

crystal potential of the crystal under consideration. Here, in

order to compare the result with that of Lafon and Lin using STO,

atomic-Hartres-Fock-Slater potential (AHFS) according to the scheme

of Woodruff[39] is used for diamond. The crystal potential is con-

sidered as the superposition of each individual free-atom potential:

$$V(\vec{r}) = \sum_{\nu} V_{atomic}(\vec{r} - \vec{R}_{\nu}), \qquad (5.8)$$

where $\vec{R}_{\nu}$ is the primitive translation vector for the atomic sites.

The atomic potential is in turn expressed as the sum of the Coulomb

and exchange contributions:

$$V_{atomic}^{Coul}(\vec{r}) = -\frac{Z}{r} + \left(\frac{4\pi}{r}\right) \int_{0}^{r} \rho(r') r'^2 dr' + 4\pi \int_{r}^{\infty} \rho(r') r' dr', \qquad (5.9)$$

$$V_{atomic}^{exch}(r) = -\frac{3}{2} [3\rho(r)/\pi]^{\frac{1}{3}}. \qquad (5.10)$$

Where Z is the atomic number, $\rho(r)$ is the atomic charge density.

In equation (5.10), Slater exchange term has been used. This term

has been subjected to various alternations in recent years.[40]

However, no attempt was made here to adopt any of those alternations

of numerical factor. It should be noted, however, the exchange

crystal potential should be the cubic root of the sum of the atomic

exchange potentials. An approximation is made here to represent the

exchange crystal potential as the sum of the cubic root of each individual free atomic potential. This procedure simplifies the calculation. In his subsequent study of diamond charge density,[41] Lafon made a comparison of these two approaches and found that the simplification is indeed justified.

For diamond, the free atomic charge density $\rho(r)$ is obtained from the Hartree-Fock self-consistent-field calculations of Jucys'.[42] The expression is

$$4\pi\rho(r) = 2[R_{1s}(r)]^2 + 2[R_{2s}(r)]^2 + 2[R_{2p}(r)]^2 , \qquad (5.11)$$

where R_{1s}, R_{2s}, and R_{2p} are the radial part of the 1s, 2s, and 2p wave functions respectively. The origin of the potential is located at the mid-point connecting the two face-centered cubic lattice. The Wigner-Seitz cell about the origin has a volume of $\Omega = \frac{1}{4}a_0^3$ and contains two atoms at the locations given by

$$\vec{t}_1 = \frac{1}{8} a_0(1, 1, 1) \qquad \text{and} \qquad \vec{t}_2 = -\vec{t}_1 ,$$

for the two face-centered cubic lattices one and two.

Then the potential can be expressed as

$$V(\vec{r}) = \sum_\nu \sum_{i=1}^{2} V_{atomic} [\vec{r} - (\vec{R}_\nu + \vec{t}_i)] , \qquad (5.12)$$

which is then expanded in the reciprocal lattice

$$V(\vec{r}) = \sum_\nu V(\vec{K}_\nu) \exp(i\vec{K}_\nu \cdot \vec{r}) . \qquad (5.13)$$

Due to the choice of the origin, the potential is invariant under the inversion operation. Equation (5.13) can be written as

$$V(\vec{r}) = \sum_\nu V(\vec{K}_\nu) \cos\vec{K}_\nu \cdot \vec{r} . \qquad (5.14)$$

The Fourier coefficients are given by

$$V(\vec{K}_\nu) = \frac{1}{N\Omega} \int V(\vec{r}) \cos\vec{K}_\nu \cdot \vec{r} \, d\tau \qquad (5.15)$$

where N is the number of unit cells in the crystal and Ω is the
volume of the unit cell. The Fourier coefficients can also be
divided into two parts: Coulomb and exchange parts. The detailed
derivation of this Fourier transformation is given in appendix B.
The result is:

$$V(\vec{K_\nu}) = -\frac{8\pi}{K^2\Omega}\cos\vec{K_\mu} \cdot \vec{t}\left\{Z - \frac{1}{K_\nu} \int_0^\infty Q(r) \sin K_\nu r\, dr\right.$$
$$\left. + K_\nu\int_0^\infty E(r)\sin K_\nu r\, dr\right\}, \tag{5.16}$$

where $Q(r) = 4\pi r\rho(r)$
$$E(r) = \frac{3}{2}r[3\rho(r)/\pi]^{\frac{1}{3}}.$$

Using $a_0 = 6.728$ a.u., Lafon and Lin generated 4409 Fourier
coefficients. The $V(0, 0, 0)$ was set at -1.435a.u. in order to
compare with the OPW calculation of Bassani and Yoshimine[43] using
the same potential. The first fifteen coefficients are listed in
Table IV.

TABLE IV

FOURIER COEFFICIENTS FOR V(r)

$\dfrac{\vec{a_o K}}{2\pi} = \vec{l}$			Fourier Coefficients
l_x	l_y	l_z	V_K
0	0	0	-1.435
1	1	1	-0.4550
2	2	0	-0.2080
3	1	1	-0.1586
4	0	0	-0.1148
3	3	1	-0.0990
4	2	2	-0.08094
3	3	3	-0.07312
5	1	1	-0.07312
4	4	0	-0.06312
5	3	1	-0.05838
6	2	0	-0.05192
5	3	3	-0.04870
4	4	4	-0.04414
5	5	1	-0.04179

CHAPTER VI

CRYSTAL SYMMETRY AND GROUP THEORY

The full symmetry group of a crystalline solid is the space
group which consists of translational-symmetry operators and
rotational-symmetry operators. The former form the pure transla-
tional subgroup and the latter form the point group. A well-known
group-theoretical principle in quantum mechanics states that the wave
functions of a quantum system must form bases for irreducible repre-
sentations of the group of operators which commute with the
Hamiltonian of the system.

A general space-group element may be written as $\{\vec{R}|\vec{t}\}$ where
$\vec{R}$ is the rotational operator of the point group and $\vec{t}$ is the trans-
lational operator of the translation group,

$$\{\vec{R}|\vec{t}\}\vec{X} = \vec{R}\vec{X} + \vec{t} . \qquad (6.1)$$

When $\vec{t} = 0$, the aggregate of the operators form the point-group.
When $\vec{R}$ is the identity operator $\vec{E}$, the aggregate of the pure trans-
lational operators form the invariant and Abelian subgroup. This
translational subgroup contains all the translations which can be
written as

$$\vec{t}_n = n_1\vec{a}_1 + n_2\vec{a}_2 + n_3\vec{a}_3 \qquad (6.2)$$

Bloch Theorem states that if we have an operator $\vec{T}_{\vec{t}}$ such

that

$$\vec{T}_{\vec{\alpha}}(\vec{r}) = \vec{r} + \vec{\alpha} \quad,$$

then for a wave function $\psi_{\vec{k}}$

$$\vec{T}_{\alpha}(\psi_{\vec{k}}) = \exp{(i\vec{k} \cdot \vec{\alpha})}\psi_{\vec{k}} \quad. \tag{6.3}$$

The Hamiltonian H belongs to the translational group with

element $\vec{T}_{\vec{t}_n}$. Since for any arbitration translation group (6.3) holds,

we can consider $\exp{(i\vec{k} \cdot \vec{t}_n)}$ as the representation of $\vec{T}_{\vec{t}_n}$, then

$$\vec{T}_{\vec{t}_n}\psi(\vec{r}) = \exp{(i\vec{k} \cdot \vec{t}_n)}\psi(\vec{r}). \tag{6.4}$$

We now label $\psi(\vec{r})$ as $\psi_{\vec{k}}(\vec{r})$, then write

$$\psi_{\vec{k}}(\vec{r}) = \exp{(i\vec{k} \cdot \vec{r})}U_{\vec{k}}(\vec{r}), \tag{6.5}$$

$$\vec{T}_{\vec{t}_n}\psi_{\vec{k}}(\vec{r}) = \exp{(i\vec{k}(\vec{r} + \vec{t}_n))}U_{\vec{k}}(\vec{r} + \vec{t}_n) \quad. \tag{6.6}$$

Therefore,

$$U_{\vec{k}}(\vec{r} + \vec{t}_n) = U_{\vec{k}}(\vec{r}), \tag{6.7}$$

and $U_{\vec{k}}$ is periodic. This satisfies the periodic property of the

crystal.

In chapter V, we have seen that a typical vector in the

reciprocal space is defined as

$$\vec{K}_m = 2\pi(m_1\vec{b}_1 + m_2\vec{b}_2 + m_3\vec{b}_3),$$

and

$$\vec{K}_m \cdot \vec{t}_n = 2\pi(m_1 n_1 + m_2 n_2 + m_3 n_3)$$
$$= 2\pi \times \text{integer}.$$

Then

$$\exp{(i(\vec{k} + \vec{K}_m) \cdot \vec{t}_n)} = \exp{(i\vec{k} \cdot \vec{t}_n)} \quad. \tag{6.8}$$

If we apply the translational operator $\vec{T}_{\vec{t}_n}$ on the wave

function $\psi_{\vec{k}} + \vec{K}_m$,

$$\vec{T}_{\vec{t}_n} \psi_{\vec{k}+\vec{K}_m} = \exp(i(\vec{k} + \vec{K}_m) \cdot \vec{t}_n)\psi_{\vec{k}+\vec{K}_m}$$

$$= \exp(i\vec{k} \cdot \vec{t}_n)\psi_{\vec{k}+\vec{K}_m}(\vec{r}) \qquad (6.9)$$

This shows that $\psi_{\vec{k}}$ and $\psi_{\vec{k}+\vec{K}_m}$ have the same symmetry property. Thus $\vec{k}$ and $\vec{K}$ are equivalent vectors in the sense as far as the relation (6.4) is concerned, $\vec{k}$ and $\vec{k} + \vec{K}_m$ are not distinguishable. Therefore we can consider them to have essentially the same $\vec{k}$ value. It is justified now that we confine all our attention to $\vec{k}$ vectors lying inside a finite zone of the k- space. This zone is known as the first Brillouin zone which is constructed by setting up perpendicular bisecting planes on lines connecting the origin to all reciprocal-lattice points and then taking the volume about the origin enclosed by these planes. The set of points $\vec{k} + \vec{K}_m$ all designates the same irreducible representations of the translation group. All of k-space can be filled by fitting together a multitude of such zones, each centered on a lattice point, in which case the energy is a periodic function k throughout the k-space. Conventionally, one chooses the wave vector $\vec{k}$ so that it always lies within the first Brillouin zone. This procedure is known as reduced zone scheme.

If $\vec{R}$ is the operator of the point group, then when we apply this operator to a wave function of Bloch form

$$\vec{R}\psi_{\vec{k}} = \vec{R}\exp(i\vec{k} \cdot \vec{r})U_{\vec{k}}(\vec{r})$$

$$= U_{\vec{k}}(\vec{R}^{-1}\vec{r})\exp(i\vec{k} \cdot \vec{R}^{-1}\vec{r}) \qquad (6.10)$$

It is seen that

$$\vec{k} \cdot \vec{R}^{-1}\vec{r} = \vec{R} \cdot \vec{k} \cdot \vec{R}\vec{R}^{-1}\vec{r}$$

$$= \vec{R} \cdot \vec{k} \cdot \vec{r} \ , \tag{6.11}$$

and the result of operation is

$$\vec{R} \, \Psi_{\vec{k}} = \exp(i\vec{R}\vec{k} \cdot \vec{r})U_{\vec{k}}(\vec{R}^{-1}\vec{r}). \tag{6.12}$$

$U_{\vec{k}}(\vec{R}^{-1}\vec{r})$ is periodic if $U_{\vec{k}}(\vec{r})$ is since if $\vec{r}$ is a primitive transla-
tion, $\vec{R}^{-1}\vec{r}$ must also be a primitive translation. Periodicity is all
that is required for $U_{\vec{k}}(\vec{r})$. Hence we may write $U_{\vec{k}}(\vec{R}^{-1}\vec{r})$ as
$U_{\vec{R}'\vec{k}}(\vec{r})$. $U_{\vec{k}}(\vec{r})$ and $U_{\vec{R}'\vec{k}}(\vec{r})$ only differ by a phase factor. The result
is that by applying an operator to the wave function, we are only
rotating the $\vec{k}$-vector. The eigenfunction is still in Bloch form.
This conclusion enables us to inspect the $\vec{k}$-vector and find out all
the symmetry-related $\vec{k}$ vectors, all of them must have associated
eigenfunction of the same energy. In other words, if Ψ is an
acceptable wave function with eigenvalue E , $\vec{R}\Psi$ is also an accept-
able wave function with the same energy.

If we start with an arbitrary $\vec{k}$-vector and apply all the
rotational operations and generate all the orientations of the
$\vec{k}$-vector, such aggregate of orientations is called a "star",[44]
and all the $\vec{k}$'s are different. However, if we place the $\vec{k}$-vector
along a pre-chosen symmetry position, then some of the $\vec{R}\vec{k}$'s are
the same. The subgroup of $\vec{R}$'s which leave $\vec{k}$ unchanged is called
the group of the wave vector. The irreducible representations of the
group are called small representations. The small group is the
subgroup of the point group.

To summarize: the translational symmetry properties of the crystal makes it possible for us to confine our discussion of the energy band structure within the first Brillouin zone. The rotational symmetry properties give us the information about the energy levels and degeneracies in the crystal.

CHAPTER VII

BASIS FUNCTIONS

The atomic wave functions have the usual form

$$\psi = \sum_i c_i \phi_{g,i} \quad , \tag{7.1}$$

where

$$\phi_{g,i} = R_n(r) Y_{lm}(\theta,\phi) \quad . \tag{7.2}$$

The radial-part of the wave functions is taken from Huzinaga's self-consistent-Hartree-Fock calculation of carbon,[45]

$$R_n(r) = N_i r^{n-1} \exp(-\alpha_i r^2) \quad , \tag{7.3}$$

where N_i, the normaligation constant is given by

$$N_i = \left[\frac{2^{2n+\frac{3}{2}}}{(2n-1)!!/\pi} \right]^{\frac{1}{2}} (\alpha_i)^{\frac{(2n+1)}{4}} \quad .$$

The coefficients C_i and the Gaussian exponential parameter α_i for 1s, 2s, and 2p orbitals of carbon are listed in Table V.

Equation (7.1) could be written more explicitly as the following expressions,

$$\psi_{1s,\,2s} = \left[8 \left(\frac{2}{\pi} \right)^{\frac{1}{2}} \right]^{\frac{1}{2}} \left\{ \sum_j c_j \alpha_j^{\frac{3}{4}} \exp(-\alpha_j r^2) \right\} Y_{0,0}(\theta,\phi), \tag{7.4a}$$

$$\psi_{2p} = \left[\frac{32 \left(\frac{2}{\pi} \right)^{\frac{1}{2}}}{3} \right]^{\frac{1}{2}} r \left\{ \sum_j c_j \alpha_j^{\frac{5}{4}} \exp(-\alpha_j r^2) \right\} Y_{1,m}(\theta,\phi). \tag{7.4b}$$

43

TABLE V

c_i AND α_i OF CARBON

$c_i(1s)$	$c_i(2s)$	$c_i(2p)$	α_i
0.43809	-0.17699		5.14773
0.15459	-0.03606		42.4974
0.04534	-0.00974		146.097
0.00934	-0.00202		634.882
0.14581	-0.05267		1.96655
0.00199	0.57408		0.49624
0.35867	-0.08938		14.1892
0.00122	-0.00026		4232.61
0.00041	0.54768		0.15331
		0.50734	0.35945
		0.30611	1.14293
		0.09150	3.98640
		0.01469	18.1557
		0.31735	0.11460

We thus have all the free atomic wave functions at our disposal to construct the basis functions for the crystal Hamiltonian, the Bloch sum.

The Bloch sum is formed from these atomic functions for each of the two sub-lattices,

$$b_\alpha^j(\vec{k}, \vec{r}) = \sum_\nu \exp(i\vec{k} \cdot \vec{R}_\nu) \psi_\alpha [\vec{r} - (\vec{R}_\nu + \vec{\tau}_j)] , \qquad (7.5)$$

where α = 1s, 2s, $2p_x$, $2p_y$, $2p_z$ and the index j indicates the sub lattice, thus $b_{1s}^1(\vec{k}, \vec{r})$ designates a 1s-Bloch sum associated with the first sub-lattice, etc. In order to avoid the complex factor in the energy matrix, it is a common practice to choose a phase factor for the Bloch sum so that the matrix elements are all real. In the case of diamond, at (0, 0, 0) in k-space which in BSW notation[44] is known as Γ-point, the calculation will be further simplified by forming "bonding" and anti-bonding" combinations,

$$b_\alpha^{\pm}(\vec{k}, \vec{r}) = I^{\mp}(\alpha)[N\Omega_\alpha^{\pm}(k)]^{-\frac{1}{2}} \sum_\nu \exp(i\vec{k} \cdot \vec{R}_\nu)$$

$$\times \left\{ \psi_\alpha[\vec{r} - (\vec{R}_\nu + \vec{t}_1)] \pm \psi_\alpha[\vec{r} - (\vec{R}_\nu + \vec{t}_2)] \right\} , \qquad (7.6)$$

the phase factor $I^{\mp}(\alpha)$ are defined as

$$I^+(\alpha) = -iI^-(\alpha) = \begin{cases} 1 & \text{for } \alpha = ns \\ i & \text{for } \alpha = np_{x, y, z} \end{cases} ,$$

and $\Omega_\alpha^{\pm}(k)$ are the normalization constants. At Γ-point, the Γ group of diamond lattice divides into the irreducible representations:

$$\Gamma_1 + \Gamma_{15} + \Gamma_{25}' + \Gamma_2'$$

where Γ_1 and Γ_2' are both singlet and Γ_{15} and Γ_{25}' are both triplet. From the transformation properties of various wave functions, it is obvious that the bonding of the s-functions forms the representation of Γ_1; anti-bonding Γ_2'. The bonding of the p-functions forms the representation of Γ_{15} and anti-bonding Γ_{25}.[46]

CHAPTER VIII

MULTICENTER INTEGRALS

In order to find the energy band, the ten Bloch functions are

used as basis for the secular equation,

$$\mid H_{nlm, \; n'l'm'}(\vec{k}) - ES_{nlm, \; n'l'm'}(\vec{k}) \mid \; = 0, \tag{8.1}$$

where H represents the one-electron Hamiltonian

$$H = -\tfrac{1}{2}\nabla^2 + V(\vec{r}) \; . \tag{8.2}$$

The matrix elements consist of the overlap, kinetic, and potential

integrals.

$$S_{ij}(\vec{k}) = \int b_i^*(\vec{k},\vec{r}) b_j(\vec{k},\vec{r}) d\tau$$

$$= [\Omega_i(\vec{k})\Omega_j(\vec{k})]^{-\frac{1}{2}} \sum_{\nu} \exp(i\vec{k}\cdot\vec{R}_\nu) \int \psi_i^*(\vec{r}) \psi_j(\vec{r}-\vec{R}_\nu) d\tau,$$

$$T_{ij}(\vec{k}) = \int b_i^*(\vec{k},\vec{r}) (-\tfrac{1}{2}\nabla^2) b_j(\vec{k},\vec{r}) d\tau$$

$$= [\Omega_i(k)\Omega_j(k)]^{-\frac{1}{2}} \sum_{\nu} \exp(i\vec{k}\cdot\vec{R}_\nu)$$

$$\times \int \psi_i^*(\vec{r}) (-\tfrac{1}{2}\nabla^2) \psi_j(\vec{r}-\vec{R}_\nu) d\tau \; ,$$

$$V_{ij}(\vec{k}) = \int b_i^*(\vec{k},\vec{r}) V(\vec{r}) b_j(\vec{k},\vec{r}) d\tau$$

$$= [\Omega_i(\vec{k})\Omega_j(\vec{k})]^{-\frac{1}{2}} \sum_{\nu} \exp(i\vec{k}\cdot\vec{R}_\nu)$$

$$\times \int \psi_i^*(\vec{r}) V(\vec{r}) \psi_j(\vec{r}-\vec{R}_\nu) d\tau \; . \tag{8.3}$$

The expressions $\int \psi_i^*(\vec{r}) \psi_j(\vec{r}-\vec{R}_\nu) d\tau$, etc., are known as the

multicenter integrals. Since the atomic orbitals ψ's are expressed

as linear combinations of Gaussians, provided that the individual

integrals involving Gaussians are evaluated, we have all the

integrals at our disposal.

Let a 1s Gaussian be placed at point A, and another 1s Gaussian at B, then the overlap integral for these two Gaussians is

$$\int \exp(-\alpha_1 r_A{}^2)\exp(-\alpha_2 r_B{}^2)d\tau$$

$$= (\frac{\pi}{\alpha_1+\alpha_2})^{\frac{3}{2}}\exp(-\frac{\alpha_1\alpha_2}{\alpha_1+\alpha_2}\overline{AB}^2) \ , \tag{8.4}$$

where $\vec{r}_A = \vec{r} - \vec{A}$ and $\vec{r}_B = \vec{r} - \vec{B}$.

Integrals involving higher orbitals can be obtained by successive differentiations of the 1s-1s integral, i.e.,

$$\int \exp(-\alpha_1 r_A{}^2)x_B\exp(-\alpha_2 r_B{}^2)d\tau$$

$$= \frac{1}{-2\alpha_2}\frac{\partial}{\partial B_x} \exp(-\alpha_1 r_A{}^2)\exp(-\alpha_2 r_B{}^2)d\tau$$

$$= -(\frac{\pi}{\alpha_1+\alpha_2})^{\frac{3}{2}} (\frac{\alpha_1}{\alpha_1+\alpha_2})\overline{AB}_x\exp(-\frac{\alpha_1\alpha_2}{\alpha_1+\alpha_2}\overline{AB}^2) \ . \tag{8.5}$$

Various integrals are listed in the appendix D.

The Hamiltonian for the potential integral has a general form of

$$V(\vec{K}_y)\cos(\vec{K}_y \cdot \vec{r}_c) \ . \tag{8.6}$$

The potential integral then assumes the form

$$\exp(-\alpha_1 r_A{}^2)\cos(\vec{K}_y \cdot \vec{r}_c)\exp(-\alpha_2 r_B{}^2)d\tau \ , \tag{8.7}$$

from chapter IV, we know that

$$\exp(-\alpha_1 r_A{}^2)\exp(-\alpha_2 r_B{}^2)$$

$$= \exp(-\frac{\alpha_1\alpha_2}{\alpha_1+\alpha_2}\overline{AB}^2)\exp(-(\alpha_1+\alpha_2)r_D{}^2)$$

$$D_i = (\alpha_1 A_i + \alpha_2 B_i)/(\alpha_1+\alpha_2); \ i = x, y, z.$$

Thus the Hamiltonian $\cos\vec{K}_\nu \cdot \vec{r}_C$ can be written

as

$$\cos\vec{K}_\nu \cdot \vec{r}_C = \cos[\vec{K}_\nu \cdot (\vec{r}_{CD} + \vec{r}_D)]$$

$$= \cos\vec{K}_\nu \cdot \vec{r}_{CD} \, \cos\vec{K}_\nu \cdot \vec{r}_D - \sin\vec{K}_\nu \cdot \vec{r}_{CD}$$

$$\times \sin\vec{K}_\nu \cdot \vec{r}_D \, . \tag{8.8}$$

The integral becomes

$$\int \exp\left(-\frac{\alpha_1\alpha_2}{\alpha_1+\alpha_2}\overline{AB}^2\right) \exp\left(-(\alpha_1+\alpha_2)r_D^2\right)$$

$$\times[\cos\vec{K}_\nu \cdot \vec{r}_{CD} \, \cos\vec{K}_\nu \cdot \vec{r}_D - \sin\vec{K}_\nu \cdot \vec{r}_{CD} \, \sin\vec{K}_\nu \cdot \vec{r}_D]d\tau \, . \tag{8.9}$$

Let I_1 be the integral

$$\int \exp\left(-(\alpha_1+\alpha_2)r_D^2\right) \cos\vec{K}_\nu \, \vec{r}_D \, d\tau \, ,$$

then I_1 can be evaluated as

$$I_1 = \int_0^\infty r_D^2 \exp\left(-(\alpha_1+\alpha_2)r_D^2\right)dr_D$$

$$\times \int \cos(K_\nu r_D \cos\theta) \, \sin\theta \, d\theta \, d\varphi$$

$$= -\frac{2\pi}{K_\nu}\int_0^\infty r_D \exp\left(-(\alpha_1+\alpha_2)r_D^2\right)dr_D \int_{K_\nu r_D}^{-K_\nu r_D} \cos u \, du$$

$$= \frac{4\pi}{K_\nu}\int_0^\infty r_D \exp\left(-(\alpha_1+\alpha_2)r_D^2\right)\sin K_\nu r_D \, dr_D$$

$$= \left(\frac{\pi}{\alpha_1+\alpha_2}\right)^{\frac{3}{2}} \exp\left(-\frac{K_\nu^2}{4(\alpha_1+\alpha_2)}\right) \tag{8.10}$$

and

$$I_2 = \int \exp\left(-(\alpha_1+\alpha_2)r_D^2\right) \sin\vec{K}_\nu \cdot \vec{r}_D \, d\tau = 0 \, .$$

Therefore:

$$\int \exp\left(-\alpha_1 r_A^2\right) V(\vec{r}) \exp\left(-\alpha_2 r_B^2\right) d\tau$$

$$= \sum_\nu V(\vec{K}\nu) \cdot \exp\left(-\frac{\alpha_1\alpha_2}{\alpha_1+\alpha_2}\overline{AB}^2\right) \left(\frac{\pi}{\alpha_1+\alpha_2}\right)^{\frac{3}{2}}$$

$$\exp\left(-\frac{K_\nu^2}{4(\alpha_1+\alpha_2)}\right) \cos\vec{K}_\nu \cdot \vec{r} \, . \tag{8.11}$$

At this point, one major difficulty arises.

This is the convergence of K_μ which is dictated primarily by the factor

$$V(K_\mu) \exp\left(-\frac{K_\mu^2}{4(\alpha_1 + \alpha_2)}\right) \quad ;$$

for cases where $(\alpha_1 + \alpha_2)$ is large, convergence is reached only after a large number of K_μ is employed which makes it almost impossible to carry out. This slow convergence arises mainly from the singularity of the crystal potential which varies like $-Z/|\vec{r} - \vec{R}_\mu|$ about each nucleus. In order to remove this difficulty we divide the crystal potential into two parts,

$$V(\vec{r}) = V_1(\vec{r}) + V_2(\vec{r}) , \qquad (8.12)$$

where $V_1(\vec{r})$ and $V_2(\vec{r})$ have the following properties.

(1) $V_1(\vec{r})$ has the full symmetry of the crystal and constructed as a superposition of "localized" contributions from each atom. Its Fourier expansion is identical to that of $V(\vec{r})$ for large K_μ and each atomic contribution is readily integrated with the Gaussian at the same center.

(2) $V_2(\vec{r})$ also has the full symmetry of the crystal but represents a relatively smooth function which converges rapidly in K_μ. Once $V_1(\vec{r})$ is known, $V_2(\vec{r})$ could be gotten by

$$V_2(\vec{r}) = V(\vec{r}) - V_1(\vec{r}) .$$

With the properties of $V_1(\vec{r})$ and $V_2(\vec{r})$ in mind, we can see that $V_1(\vec{r})$ behaves like $-Z/|\vec{r} - \vec{R}_\mu|$ about each nucleus. $V_2(\vec{r})$, which is a relatively smooth function of r, can be expanded in a rapidly convergent series,

$$\langle G(\alpha_1, \vec{r}_A) |V_2(\vec{r})| G(\alpha_2, \vec{r}_B) \rangle$$

$$= \sum_{\nu} a_{\nu} \langle G(\alpha_1, \vec{r}_A) |\cos \vec{K}_{\nu} \vec{r}| G(\alpha_2, \vec{r}_B) \rangle \quad . \tag{8.13}$$

The details about the convergence will be given in appendix C.

On the other hand, $V_1(\vec{r})$ is now expanded in the direct space as a superposition of function $\mathcal{U}$ centered at each site,

$$\langle G(\alpha_1, \vec{r}_A| V_1(\vec{r})| G(\alpha_2, \vec{r}_B) \rangle \quad . \tag{8.14}$$

$$= \sum_{\mu} \langle G(\alpha_1, \vec{r}_A| \mathcal{U}(\vec{r} - \vec{R}_{\mu})| G(\alpha_2, \vec{r}_B) \rangle \quad . \tag{8.14}$$

The only restriction upon $\mathcal{U}(\vec{r})$ is that it reproduces $-Z\big/|\vec{r} - \vec{R}_{\mu}|$ near the origin. We are free to choose the form of $\mathcal{U}$ for the region away from the origin in such a way to facilitate the calculation. By making $\mathcal{U}(r)$ negligibly small before it reaches the next neighbor, one can improve the summation. The particular form of $\mathcal{U}(\vec{r})$ employed is

$$\mathcal{U}(r) = -(Z/r)(1 + \gamma r^2) \exp(-\gamma r^2), \tag{8.15}$$

with $\gamma = 2.5$. For the case where both Gaussians centered at the same center and $\alpha_1 + \alpha_2 > 40$,

$$\langle G(\alpha_1, \vec{r}_A) |V_1(\vec{r})| G(\alpha_2, \vec{r}_A) \rangle \quad \text{may be approximated by}$$

$$\simeq \langle G(\alpha_1, \vec{r}_A) |\mathcal{U}(\vec{r}_A)| G(\alpha_2, \vec{r}_A) \rangle \quad . \tag{8.16}$$

where A and B refer to two different sites, the only non-negligible integrals of V_1 for $\alpha_1 + \alpha_2 > 40$ occur when $\alpha_1 \gg \alpha_2$ or $\alpha_2 \gg \alpha_1$. The approximation used are

$$\langle G(\alpha_1, \vec{r}_A) |V_1(\vec{r})| G(\alpha_2, \vec{r}_B) \rangle$$

$$\simeq \langle G(\alpha_1, \vec{r}_A) |\mathcal{U}(\vec{r}_A)| G(\alpha_2, \vec{r}_B) \rangle \quad \text{for } \alpha_1 \gg \alpha_2 \tag{8.17}$$

$$\simeq \langle G(\alpha_1, \vec{r}_A) |\mathcal{U}(\vec{r}_B)| G(\alpha_2, \vec{r}_B) \rangle \quad , \quad \text{for } \alpha_2 \gg \alpha_1 \quad \cdot \quad .$$

In actual calculation, for the case $\alpha_1 \gg \alpha_2$ we expand $G(\alpha_2, \vec{r}_B)$ about point A in Taylor series and equation (8.17) can be readily integrated out. The validity of this approximation is borne out by the fact that for the single-center integral, $\alpha_1 = 4232.61$ and $\alpha_2 = 4232.61$, this cut-off procedure gives the $(1s|V|1s)$ integral as -0.4392×10^{-2} while a rigorous summation of 1000 K_ν's gives -0.4391×10^{-2} and a summation of 3000 K_ν's gives -0.4386×10^{-2}. For the high-low combinations, we tested the pair with $\alpha_1 = 42.4974$ and $\alpha_2 = 0.15331$, a rigorous summation of K_ν's takes 944 K_ν's before it reaches convergence and gives the $(1s|V|1s)$ integral value as $-0.22862507 \times 10^{-1}$ and the cut-off procedures gives $-0.22869800 \times 10^{-1}$. From these figures, it is established that the approximation used here is indeed justified. The detail of the expansion scheme is also given in appendix C.

CHAPTER IX

RESULT AND DISCUSSION

In this calculation, all the necessary integrals are
evaluated by the method described in the previous chapter. It is
found that a big reduction of time is obtained by going from STO to
GTO even though the latter has a much larger number of basis func-
tions, i.e., in the STO calculation of diamond band structure, six
STO exponential parameters are used which results in a total of
21 integrals. In the GTO calculation, 14 GTO Gaussian parameters
are used and 105 integrals are evaluated. Even though the number
of integrals to be evaluated in the GTO formulation is five times
tue number of integrals required in the STO, the total computa-
tional time of the GTO approach is still far less than the STO
method. The results and their comparison with the STO calculation
are listed in tables VI - VIII. It is seen that they agree with
each other very well.

TABLE VI

COMPARISON OF GTO AND STO AT SYMMETRY POINTS
(ENERGY IN a.u.)

	STO	GTO
Γ_1	-0.743	-0.734
Γ_{25}'	0.0	0.0
Γ_{15}'	+0.230	+0.232
Γ_2'	+0.494	+0.494
X_1	-0.446	-0.437
X_4	-0.217	-0.205
X_1	+0.296	+0.321
X_3	+0.597	+0.593
L_2'	-0.553	-0.553
L_1	-0.452	-0.419
L_3	-0.100	-0.096
L_1	+0.368	+0.371
L_3	+0.369	+0.371
L_2'	+0.653	+0.657

TABLE VII

COMPARISON OF OPTICAL TRANSITIONS OF DIAMOND

(ENERGY IN eV)

Transition	Experi-ment[54]	STO[34]	GTO
$\Gamma_{25}{}' - \Gamma_{15}$	7.3	6.3	6.3
$\Sigma_2 - \Sigma_3$ $X_4 - X_1$	12.2	13.9	14.1
$X_1 - X_1$	16	20.1	20.6
$\Gamma_{25}{}' - \Gamma_1$	23	20.2	20.2

TABLE VIII

COMPARISON OF THE BAND STRUCTURE OF STO AND GTO

(ENERGY IN a.u.)

K_x	Basis	0.0	0.1	0.2	0.4	0.5	0.6	0.75	0.9	1.0
$\Delta_1^{(1)}$	STO	-1.243	-1.240	-1.230	-1.189	-1.160	-1.124	-1.062	-0.990	-0.938
	GTO	-1.238	-1.235	-1.225	-1.185	-1.156	-1.122	-1.061	-0.991	-0.941
$\Delta_5^{(1)}$	STO	-0.503	-0.514	-0.542	-0.608	-0.637	-0.662	-0.690	-0.704	-0.707
	GTO	-0.504	-0.516	-0.543	-0.609	-0.639	-0.664	-0.691	-0.707	-0.709
$\Delta_{2'}^{(1)}$	STO	-0.503	-0.511	-0.534	-0.612	-0.661	-0.714	-0.799	-0.883	-0.938
	GTO	-0.504	-0.513	-0.536	-0.615	-0.665	-0.719	-0.804	-0.887	-0.941
$\Delta_1^{(2)}$	STO	-0.273	-0.272	-0.271	-0.278	-0.281	-0.279	-0.261	-0.225	-0.192
	GTO	-0.272	-0.272	-0.274	-0.280	-0.280	-0.275	-0.256	-0.219	-0.189
$\Delta_5^{(2)}$	STO	-0.273	-0.257	-0.219	-0.115	-0.062	-0.012	+0.049	+0.085	+0.092
	GTO	-0.272	-0.257	-0.220	-0.119	-0.066	-0.017	+0.045	+0.082	+0.089
$\Delta_{2'}^{(2)}$	STO	-0.009	-0.005	+0.003	+0.009	-0.002	-0.026	-0.084	-0.151	-0.192
	GTO	-0.010	-0.007	+0.001	+0.009	-0.001	-0.022	-0.076	-0.142	-0.183

TABLE VIII (Continued)

K_x	Basis	0.0	0.1	0.2	0.4	0.5	0.6	0.75	0.9	1.0
$\sum_1 (1)$	STO	-1.243	-1.237	-1.216	-1.138	-1.084	-1.026	-0.955		
	GTO	-1.238	-1.231	-1.211	-1.136	-1.085	-1.029	-0.961		
$\sum_3 (1)$	STO	-0.503	-0.535	-0.601	-0.739	-0.798	-0.847	-0.902		
	GTO	-0.504	-0.536	-0.603	-0.742	-0.802	-0.851	-0.906		
$\sum_1 (2)$	STO	-0.503	-0.525	-0.575	-0.691	-0.741	-0.780	-0.791		
	GTO	-0.504	-0.527	-0.577	-0.694	-0.743	-0.780	-0.791		
$\sum_2$	STO	-0.503	-0.507	-0.521	-0.571	-0.604	-0.637	-0.678		
	GTO	-0.504	-0.509	-0.522	-0.572	-0.605	-0.639	-0.680		
$\sum_4$	STO	-0.273	-0.265	-0.242	-0.163	-0.114	-0.052	+0.029		
	GTO	-0.272	-0.265	-0.244	-0.166	-0.113	-0.056	+0.024		
$\sum_1 (3)$	STO	-0.273	-0.249	-0.200	-0.076	-0.014	+0.023	-0.023		
	GTO	-0.272	-0.251	-0.204	-0.077	-0.014	+0.022	-0.022		
$\sum_3 (2)$	STO	-0.273	-0.245	-0.196	-0.139	-0.136	-0.144	-0.168		
	GTO	-0.272	-0.247	-0.199	-0.142	-0.136	-0.142	-0.163		

56

TABLE VIII (Continued)

K_x	Basis	0.0	0.1	0.2	0.4	0.5	0.6	0.75	0.9	1.0
$\Sigma_3(3)$	STO	-0.009	-0.001	+0.017	+0.057	+0.068	+0.076	+0.086		
	GTO	-0.010	-0.003	+0.014	+0.054	+0.065	+0.072	+0.081		
$\Lambda_1(1)$	STO	-1.243	-1.233	-1.203	-1.093	-1.052				
	GTO	-1.238	-1.228	-1.200	-1.095	-1.057				
$\Lambda_1(2)$	STO	-0.503	-0.557	-0.661	-0.872	-0.927				
	GTO	-0.504	-0.558	-0.664	-0.872	-0.923				
$\Lambda_3(1)$	STO	-0.503	-0.518	-0.547	-0.592	-0.598				
	GTO	-0.504	-0.519	-0.549	-0.594	-0.600				
$\Lambda_3(2)$	STO	-0.273	-0.251	-0.206	-0.139	-0.132				
	GTO	-0.272	-0.251	-0.209	-0.141	-0.133				
$\Lambda_1(3)$	STO	-0.273	-0.234	-0.183	-0.137	-0.132				
	GTO	-0.272	-0.237	-0.186	-0.142	-0.133				
$\Lambda_1(4)$	STO	-0.009	+0.003	+0.028	+0.125	+0.148				
	GTO	-0.01	+0.0001	+0.032	+0.132	+0.153				

57

CHAPTER X

THE ENERGY BAND GAP OF MAGNESIUM OXIDE

CRYSTAL STRUCTURE

The crystal structure of magnesium oxide (MgO) is same as that of rock-salt. It is composed of two interpenetrating face-centered cubic lattices. One fcc lattice consists of oxygen atoms while the other consists of magnesium atoms. These two fcc lattices are displaced by half lattice constant a_0 along the body diagonal. The a_0 for MgO is 4.21A.

CRYSTAL POTENTIAL

The crystal potential adopted for this calculation is again the AHFS potential. The MgO lattice belongs to the point group O_h^5. The positions of Mg and O atoms in the unit all are given by

$$\vec{t}_1 = a_0(0,\ 0,\ 0)\ ,\qquad \vec{t}_2 = \frac{a_0}{2}(1,\ 1,\ 1)\ .$$

The crystal potential $V(\vec{r})$ again can be expanded in the reciprocal lattice with reciprocal lattice vector $\vec{K}_\nu$,

$$V(\vec{r}) = \sum_\nu V(\vec{K}_\nu)\ \exp(-i\vec{K}_\nu.\vec{r})\ .$$

Now we center the potential at either one of the atoms. The choice of the origin gives us a real energy matrix since the inversion symmetry is preserved. $V(\vec{K}_\nu)$ can be evaluated as,

58

$$V(\vec{K_\nu}) = \frac{1}{N\Omega} \sum_\mu \sum_{i=1}^{2} \int V_i(\vec{r} - (\vec{R_\mu} + \vec{t_i})) \exp(-i\vec{K_\nu} \cdot \vec{r}) d\tau$$

$$= \frac{1}{\Omega} \sum_{i=1}^{2} \int V_i(\vec{r} - \vec{t_i}) \exp(-i\vec{K_\nu} \cdot \vec{r}) d\tau$$

$$= \frac{1}{\Omega} \sum_{i=1}^{2} \int (V_i(\vec{r} - \vec{t_i}) \exp(-i(\vec{K_\nu} \cdot (\vec{r} - \vec{t_i}))) \exp(-i\vec{K_\nu} \cdot \vec{t_i}) d\tau$$

$$= \frac{1}{\Omega} \sum_{i=1}^{2} \int V_i(\vec{r}) \exp(-i\vec{K_\nu} \cdot \vec{r}) d\tau \exp(-i\vec{K_\nu} \cdot \vec{t_i})$$

$$= \frac{1}{\Omega} \left\{ \int V_1(\vec{r}) \cos\vec{K_\nu} \cdot \vec{r} d\tau + \cos\vec{K_\nu} \cdot \vec{t_2} \quad V_2(\vec{r}) \cos\vec{K_\nu} \cdot \vec{r} d\tau \right\} . \quad (10.1)$$

The potential now is divided into two kinds: the symmetric and anti-symmetric parts. The Fourier coefficients are:

$$V^S(\vec{K_\nu}) = \frac{1}{\Omega}[\int V_1(\vec{r}) \cos\vec{K_\nu} \cdot \vec{r} d\tau + \int V_2(\vec{r}) \cos\vec{K_\nu} \cdot \vec{r} d\tau] ;$$

for K_x, K_y and K_z all even $\quad (10.2)$

$$V^A(\vec{K_\nu}) = \frac{1}{\Omega}[\int V_1(\vec{r}) \cos\vec{K_\nu} \cdot \vec{r} d\tau - \int V_2(\vec{r}) \cos\vec{K_\nu} \cdot \vec{r} d\tau] ;$$

for K_x, K_y, and K_z all odd. $\quad (10.3)$

In the calculation, we take Mg as 1 and 0 as 2, therefore

$$V^S(\vec{K_\nu}) = V^{Mg}(\vec{K_\nu}) + V^0(\vec{K_\nu})$$

$$V^A(\vec{K_\nu}) = V^{Mg}(\vec{K_\nu}) - V^0(\vec{K_\nu}),$$

where

$$V^{Mg}(\vec{K_\nu}) = \frac{1}{\Omega} \int V_1(\vec{r}) \cos\vec{K_\nu} \cdot \vec{r} d\tau \quad (10.4)$$

$$V^0(\vec{K_\nu}) = \frac{1}{\Omega} \int V_2(\vec{r}) \cos\vec{K_\nu} \cdot \vec{r} d\tau. \quad (10.5)$$

The evaluation of these coefficients are the same as the case of diamond we tabulate the first fifteen $V^{Mg}(\vec{K_\nu})$ and $V^0(\vec{K_\nu})$ in table IX. The atomic wave functions used are given by Clementi.[47]

WAVE FUNCTIONS

For the free oxygen atomic wave function, Stewart's small Gaussian expansion[48] is much preferable since it contains less number of Gaussians and each Gaussian is of moderate size as compared to the ones in Huzinaga's paper. The c_i's and α_i's are listed in Table X. For 3s and 3p states, we use Hosoya's[49] HF calculation of STO and fit them with the least square fitting.[50] The results are,

$$\psi_{3s} = (\tfrac{1}{4\pi})^{\frac{1}{2}} \sum_i \beta_i \exp(-\alpha_i r^2) \tag{10.6}$$

$$\psi_{3p} = (\tfrac{3}{4\pi})^{\frac{1}{2}} \sum_i \beta_i \exp(-\alpha_i r^2) . \tag{10.7}$$

The various β_i's and α_i's are tabulated in Table XI.

For magnesium, the 1s, 2s, 3s, 2p wave functions are taken from Veillard's calculations.[36] The c_i's and α_i's are tabulated in Table XII. The 3p state are taken from the tabulated values by Trefftz and Bierman[51] who used the HFSCF scheme to calculate the wave functions. The β_i's and α_i's are tabulated in Table XIII.

We therefore have all the free atomic wave functions at our disposal to construct the basis functions for the crystal Hamiltonian — the Bloch sum.

The Bloch functions are constructed in the usual manner as

$$b_{nlm}(\vec{k},\vec{r}) = [N\Omega(\vec{k})]^{-\frac{1}{2}} \sum_\nu \exp(-i\vec{k}\cdot\vec{R}_\nu)$$
$$\times \psi_{nlm}(\vec{r}-\vec{R}_\nu) . \tag{10.8}$$

The energy matrix is set up by 1s, 2s, 3s, 2p, 3p functions of both magnesium and oxygen and all the multicenter integrals are evaluated in the same manner as before. The same "cut-off" procedure with a

little revision is employed. The details are given in Appendix C. The 18x18 energy matrix is diagonalized at the Γ-point.

RESULT AND DISCUSSION

At the Γ-point, the energy levels splits into ten levels four of them are triplets. They are tabulated in Table XIV. We can identify Γ_A, Γ_B, Γ_C and Γ_D as the Mg 1s, oxygen 1s, Mg 2s, Mg 2p core states respectively. Γ_F corresponds to experimental value[29] at Γ_{15} and is the top of the valence band. Γ_G corresponds to their Γ_1 which is the bottom of conduction band. The band gap is 10.7 eV vs. the experimental value of 7.8 eV. The existence of Γ_E and Γ_H at their respective positions have not been confirmed by experimental data. Since there are no other first principle calculations that we know of at present time, no conclusion can be drawn about this point. It is suggested that a SCF approach be applied to this problem and further ascertain the exact positions of these levels. In view of the computer time involved, a complete band analysis should be followed only after the problem at Γ-point is resolved. Despite the difficulty cited here, the LCAO method does give fairly good agreement between the theoretical and experimental band gap values. This points out the fact that with an improved crystal potential, the LCAO method is able to yield better result.

TABLE IX

FOURIER COEFFICIENTS FOR $V^{Mg}(\vec{r})$ AND $V^0(\vec{r})$

$\dfrac{a_o \vec{K}}{2\pi} = \vec{1}$			$V_{K_\nu}^{Mg}$	$V_{K_\nu}^0$
1_x	1_y	1_z		
0	0	0	-1.0000	-1.0000
1	1	1	-0.22965	-0.19667
2	0	0	-0.19500	-0.16307
2	2	0	-0.12893	-0.10146
3	1	1	-0.10421	-0.080168
2	2	2	-0.97981	-0.074982
4	0	0	-0.079098	-0.059642
3	3	1	-0.069162	-0.051742
4	2	0	-0.066400	-0.049559
4	2	2	-0.057348	-0.042417
3	3	3	-0.052114	-0.038295
5	1	1	-0.052114	-0.038295
4	4	0	-0.045385	-0.032988
5	3	1	-0.042205	-0.030473
4	4	2	-0.041252	-0.029720

TABLE X

C_i AND α_i OF OXYGEN

C_i (1s)	C_i (2s)	C_i (2p)	α_i
0.137884	-0.0297337		149.926
0.481402	-0.145386		27.1311
0.502395	-0.194778		7.18802
0.0351062	0.618588		0.91247
-0.00978845	0.499792		0.272406
		0.0138204	41.6051
		0.122175	7.40821
		0.382355	1.87952
		0.487390	0.56275
		0.253299	0.177164

TABLE XI

β_i AND α_i OF OXYGEN

$\beta_i(3s)$	$\beta_i(3p)$	α_i
-0.395933	-0.00448594	0.177164
-0.234483		1.87952
-0.686843	0.121193	0.56275
0.42302		0.272406
0.386842		7.18802
0.728111		27.1311
0.051912	-0.00706031	0.01506
0.295691		0.91247
0.723929		149.926
0.169199	-0.00322285	0.004045
	0.401516	1.87952
	0.432280	7.40821
	0.295612	41.16051

TABLE XII

C_i AND α_i OF Mg

$C_i(1s)$	$C_i(2s)$	$C_i(3s)$	$C_i(2p)$	α_i
0.00038	-0.00009	0.00001		43643.6
0.00293	-0.00073	0.00014		6585.89
0.01496	-0.00384	0.00074		1510.32
0.05863	-0.01514	0.00291		431.833
0.17661	-0.04979	0.00971		142.071
0.37113	-0.11832	0.002298		51.4089
0.40079	-0.20111	0.04123		19.9361
0.12384	-0.02310	0.00306		8.04158
0.00375	0.57420	-0.13501		2.50948
0.00052	0.53517	-0.25490		0.871939
-0.00003	0.02118	0.59531		0.108819
0.00001	0.00801	0.52058		0.040455
			0.00475	192.644
			0.03462	45.7493
			0.14372	14.2558
			0.34665	4.99324
			0.46489	1.78234
			0.24109	0.61510

TABLE XIII

β_i AND α_i OF Mg

β_i(3p)	α_i
-0.0039006	0.01506
-0.0361927	0.040455
-0.146854	0.177164
0.233841	0.272406
-0.642646	0.6151
0.931061	0.871939
-1.11535	1.78234
1.44632	2.50948
-0.0480317	4.99324
1.67100	1.42558

TABLE XIV

Γ-POINT ENERGY LEVELS OF MgO

Γ	E in a.u.
Γ_A(singlet)	-48.758
Γ_B(singlet)	-20.865
Γ_C(singlet)	- 4.20029
Γ_D(triplet)	- 2.97507
Γ_E(singlet)	- 2.12606
Γ_F(triplet)	- 2.05207
Γ_G(singlet)	- 1.64585
Γ_H(triplet)	- 1.54222
Γ_I(triplet)	- 5.37088
Γ_J(singlet)	2.67848

APPENDIX A

DERIVATION OF $S_2(b)$ FOR DIPOLE-DIPOLE INTERACTION

For dipole-dipole interaction, the $S_2(b)_{o,i}$ term is given by

$$S_2(b)_{o,i} = \frac{4}{9} \left(\frac{P_1 P_2}{\hbar v} \right)^2 \frac{1}{b^4} \sum_{j_1, j_2} (j_1 1 K_1 0 | j_1, K_1)^2$$

$$\times (j_2 1 K_2 0 | j_2, K_2)^2 f_1(k) \tag{A.1}$$

according to the selection rule

$$j_i + 1 \qquad\qquad j_2 + 1$$

$$j_{i'} = j_i \qquad \text{and} \quad j_2 = j_2$$

$$j_i - 1 \qquad\qquad j_2 - 1 \tag{A.2}$$

Therefore we have nine different matrix elements; namely,

$$(j_i 1 K_i 0 \; j_i + 1 \; K_i)^2 \qquad (j_2 1 K_2 0 \; j_2 + 1 \; K_2)^2$$

$$x$$

$$(j_i 1 K_i 0 \; j_i \; K_i)^2 \qquad (j_2 1 K_2 0 \; j_2 K_2)^2$$

$$(j_i 1 K_i 0 \; j_i - 1 \; K_i)^2 \qquad (j_2 1 K_2 0 \; j_2 - 1 \; K_2)^2$$

using the table for C - G coefficients,[20] these nine different

coefficients can be evaluated. $f_1(k)$ is defined in (2.26) with

$$k = \frac{2}{v} \frac{b}{} B[j_i(j_i' + 1) - j_i(j_i + 1) + j_2' + 1) - j_2(j_2 + 1)].$$

Define $x = \frac{4 \pi b B}{v}$ and $k = xD$,

the transitions are classified as:

for $\Delta j_1 = 0$, $\Delta j_2 = 0$, $D = 0$,

$$S_2(b)_{0,i} = (j_1 1 K_1 0 | j_1 K_i)^2 (j_2 1 K_2 0 | j_2 K_2)^2$$

$$= \frac{K_1^2}{J_1(J_1+1)} \frac{K_1^2}{J_2(J_2+1)}$$

$$S_2(b)_{0,f} = \frac{K_1^2}{(J_1+1)(J_1+2)} \frac{K_2^2}{J_2(J_2+1)}$$

$$S_2(b)_m = (-1)^{j_i + j_f + 1} \frac{8}{9} \left(\frac{P_1 P_2}{\hbar v}\right)^2 \frac{1}{b^4}$$

$$x \sqrt{(2j_i+1)(2j_f+1)} \quad (j_i 1 K_i 0 | j_i K_i)$$

$$x \ (j_f 1 K_f 0 | j_f K_f) W(j_i j_f j_i j_f, 11)$$

$$\sum_{j_2'} (j_2 1 K_2 0 | j_2, K_2)^2 \ f_i(k)$$

where $W(j_i j_f j_i j_f, 11)$ is the Racah coefficients the value of it can be found in reference 21. In our case

$\quad W(abcd; if) \quad$ with $f = 1$ and $a = b - 1$, $c = d - 1$:

$\quad W(abcd; 11) = (-1)^{b+d-f}$

$$x \left[\frac{(f+b+d+1)(f+b+d)(-f+b+d)(-f+b+d-1)}{4(ab+1)b(2b-1)(2d+1)d(ad-1)}\right]^{\frac{1}{2}}.$$

We see that $S_2(b)_m$ exists only when $\Delta j_i = 0$, i.e., only diagonal matrix elements exist. The $S_2(b)_m$ in this case is given by:

$$S_2(b)_m = -\frac{4}{9}\left(\frac{P_1 P_2}{\hbar v}\right)^2 \frac{1}{b^4} \frac{K_i K_f}{(J_i+1)^2}.$$

Therefore for $\Delta J_i = 0$, $\Delta J_2 = 0$,

$$S \ (b) = \frac{4}{9} \left(\frac{P_1 P_2}{\hbar v}\right)^2 \frac{1}{b^4} \frac{K_2^2}{J_2(J_2+1)} \left[\frac{K_1^2}{J_1(J_1+1)}\right.$$

$$\left. + \frac{K_1^2}{(J_1+1)(J_1+2)} \frac{K_1^2}{(J_1+1)^2}\right].$$

$$\Delta J_i = 1, \quad \Delta J_2 = -1, \quad D = J_i - J_2 + 1,$$

$$S_{inel_1}{}^{(b)}{}_{o,i} = \frac{4}{9} \left(\frac{P_1 P_2}{\hbar v}\right)^2 \frac{1}{b^4} \left(j_i 1 K_i 0 | j_i + 1 K_i\right)^2$$

$$\times \left(j_2 1 K_2 0 | j_2 - 1 K_2\right)^2 f_4\{x(J_i - J_2 + 1)\}$$

$$= \frac{4}{9} \left(\frac{P_1 P_2}{\hbar v}\right)^2 \frac{1}{b^4} \left\{ \frac{J_2{}^2 - K_2{}^2}{J_2(2J_2 + 1)} \right.$$

$$\frac{(J_1 + 1)^2 - K_i{}^2}{(2J_1 + 1)(J_1 + 1)} f_1\{x(J_1 - J_2 + 1)\} \right\}$$

$$S_{inel_1}{}^{(b)}{}_{o,f} = \frac{4}{9} \left(\frac{P_1 P_2}{\hbar v}\right)^2 \frac{1}{b^4} \left\{ \frac{K_2{}^2 - K_2{}^2}{J_2(2J_2 + 1)} \right.$$

$$\frac{(J_1 + 2)^2 - K_1{}^2}{(2J_1 + 1)(J_1 + 1)} f_1\{x(J_1 - J_2 + 2)\} \right\}$$

$$\Delta J_i = -1, \quad \Delta J_2 = 1, \quad D = J_2 - J_i + 1,$$

$$S_{inel_2}{}^{(b)}{}_{o,i} = \frac{4}{9} \left(\frac{P_1 P_2}{\hbar v}\right)^2 \frac{1}{b^4} \left(j_i 1 K_i 0 | j_i - 1 K_i\right)^2$$

$$\times \left(j_2 1 K_2 0 | j_2 + 1 K_2\right)^2 f_1\{x(J_2 - J_i + 1)\}$$

$$= \frac{4}{9} \left(\frac{P_1 P_2}{\hbar v}\right)^2 \frac{1}{b^4} \left\{ \frac{(J_1 - K_1)(J_1 + K_1)}{J_1(2J_1 + 1)} \right.$$

$$\times \frac{(J_2 + 1)^2 - K_1{}^2}{(2J + 1)(J + 1)} \times f_i\{x(J_2 - J_1 + 1)\} \right\}$$

$$S_{inel_2}{}^{(b)}{}_{0,f} = \frac{4}{9} \left(\frac{P_1 P_2}{\hbar v}\right)^2 \frac{1}{b^4} \left\{ \frac{(J_1 + 1)^2 - K_1{}^2}{(J_1 + 1)(2J_1 + 3)} \right.$$

$$\times \frac{(J_2 + 1)^2 - K_1{}^2}{(2J + 1)(J + 1)} f_1\{x(J_2 - J_1)\} \right\}$$

$$S_{inel} = \frac{4}{9} \left(\frac{P_1 P_2}{\hbar v} \right)^2 \frac{1}{b^4} \left\{ \frac{(J_2-K_2)(J_2+K_2)}{J_2(2J_2+1)} \right.$$

$$\left[\frac{(J_1+1)^2-K_1^2}{(2J_1+1)(J_1+1)} \; f_1 \left\{ x(J_1-J_2+1) \right\} \right.$$

$$\left. + \frac{(J_1+2)^2-K_1^2}{(2J_1+3)(J_1+2)} \; f_1 \quad x(J_1-J_2+2) \right\} \;]$$

$$+ \frac{(J_2+1)^2-K_2^2}{(2J+1)(J+1)} \; [\; \frac{J_1^2-K_1^2}{J_1(2J_1+1)} \; f_1 \left\{ x(J_2-J_1+1) \right\}$$

$$+ \frac{(J_1+1)^2-K_1^2}{(J_1+1)(2J_1+3)} \; f_1 \left\{ x(J_2-J_1) \right\} \;] \right\}$$

$$\Delta J_i = 1 \quad \Delta J_2 = 0 \quad D = J_i + 1$$

$$S'_{inel_1}(b)_{o,i} = \frac{4}{9} \left(\frac{P_1 P_2}{\hbar v} \right)^2 \frac{1}{b^4} \; (j_i 1 K_i 0 | j_i+1 \; K_i)^2$$

$$(j_2 1 K_2 0 | J_2 K_2)^2 \; f_1 \{ x(J_i+1) \}$$

$$= \frac{4}{9} \left(\frac{P_1 P_2}{\hbar v} \right)^2 \frac{1}{b^4} \; \frac{K_2^2}{J(J+1)}$$

$$\frac{(J_1+2)^2-K_1^2}{(2J_1+3)(J_1+2)} \; f_1 \{ x(J_1+2) \}$$

$$\Delta J_i = -1, \; \Delta J_2 = 0, \quad D = J_i,$$

$$S'_{inel_2}(b)_{o,i} = \frac{4}{9} \left(\frac{P_1 P_2}{\hbar v} \right)^2 \frac{1}{b^4} \; (j_i 1 K_i 0 | j_i - 1 K_i)^2$$

$$(j_2 1 K_2 0 | j_2 K_2)^2 \; f_1 \{ x J_i \}$$

$$= \frac{4}{9} \left(\frac{P_1 P_2}{\hbar v} \right) \frac{1}{b^4} \; \frac{K_2^2}{J_2(J_2+1)} \quad \frac{J^2-K^2}{J(J+1)}$$

$$f_1 (x J_1)$$

$$S'_{inel_2}{}^{(b)}{}_{o,f} = \frac{4}{9} \left(\frac{P_1 P_2}{\hbar v} \right)^2 \frac{1}{b^4} \frac{K_2^2}{J_2(J_2+1)}$$

$$\frac{(J+1)^2 - K_1^2}{(J_1+1)(2J_1+3)} f_1\{x(J_1+1)\}$$

$$\Delta J_i = 0, \quad \Delta J_2 = 1, \quad D = J_2 + 1$$

$$S'_{inel_3}{}^{(b)}{}_{o,i} = \frac{4}{9} \left(\frac{P_1 P_2}{\hbar v} \right)^2 \frac{1}{b^4} (j_i 1 K_i 0 | j_i K_i)^2$$

$$(j_2 1 K_2 0 | j_2 + 1 \, K_2) \quad f_1(x(J_2+1))$$

$$S'_{inel_3}{}^{(b)}{}_m = (-1)^{j_i + j_f + 1} \frac{8}{9} \left(\frac{P_1 P_2}{\hbar v} \right)^2 \frac{1}{b^4}$$

$$x \quad \sqrt{(2J_i+1)(2J_f+1)} \, (j_i 1 K_i 0 \; j_i K_i)$$

$$x \quad (j_f 1 K_f 0 | j_f K_f) W(j_i j_f j_i j_f, \; 11)$$

$$x \quad (j_2 1 K_2 0 | j_2 + 1 K_2)^2 \; f_1(x(J_2+1))$$

$$S'_{inel_3}{}^{(b)}{}_{o,i} = \frac{4}{9} \left(\frac{P_1 P_2}{\hbar v} \right)^2 \frac{1}{b^4} \frac{(J_2+1) - K_2^2}{(2J+1)(J+1)}$$

$$\frac{K_1^2}{J_1(J_1+1)} \; f_1(x(J_2+1))$$

$$S'_{inel_3}{}^{(b)}{}_{o,f} = \frac{4}{9} \left(\frac{P_1 P_2}{\hbar v} \right)^2 \frac{1}{b^4} \frac{(J_2+1)^2 - K_2^2}{(2J_2+1)(J_2+1)}$$

$$\frac{K_1^2}{(J_1+1)(J_1+2)} \; f_1(x(J_2+1))$$

$$S'_{inel_3}{}^{(b)}{}_m = \frac{4}{9} \left(\frac{P_1 P_2}{\hbar v} \right)^2 \frac{1}{b^4} (-1) \frac{2K_1^2}{(J_1+1)^2}$$

$$\frac{(J_2+1)^2 - K_2^2}{(2J_2+1)(J_2+1)} \; f(x(J_2+1))$$

$$S'_{inel_3}(b) = \frac{4}{9} \left(\frac{p_1 p_2}{\hbar v} \right)^2 \frac{1}{b^4} \frac{(J_2+1)^2 - K_2}{(2J+1)(J+1)} \left(\frac{K_1^2}{J_1(J_1+1)} \right.$$

$$\left. + \frac{K_1^2}{(J_1+1)(J_1+2)} - \frac{2K_1^2}{(J_1+1)^2} \right) f_1(x(J_2+1))$$

$$\Delta J_1 = o, \quad \Delta J_2 + -1, \qquad D = J_2,$$

$$S'_{inel_4}(b)_{o,i} = \frac{4}{9} \left(\frac{p_1 p_2}{\hbar v} \right)^2 \frac{1}{b^4} (j_1 1 K_2 0 \mid j_1 K_1)^2$$

$$x \ (j_2 1 K_2 0 \mid j_2 - 1 K_2)^2 \ f(x J_2)$$

$$S'_{inel_4}(b)_m = (-1)^{j_i + j_f + 1} \frac{8}{9} \left(\frac{p_1 p_2}{\hbar v} \right)^2 \frac{1}{b^4}$$

$$x \sqrt{(2J_1+1)(2J_f+1)} \ (j_1 1 K_1 0 \mid j_1 K_1)$$

$$x (j_f 1 K_f 0 \mid j_f K_f) W(j_1 j_f j_1 j_f, \ 11)$$

$$x (j_2 1 K_2 0 \mid j_2 - 1 \ K_2)^2 \ f(x J_2)$$

$$S'_{inel_4}(b)_{o,i} = \frac{4}{9} \left(\frac{p_1 p_2}{\hbar v} \right)^2 \frac{1}{b^4} \frac{J_2^2 - K_2^2}{J_2(2J_2+1)}$$

$$x \ \frac{K_1^2}{J_1(J_1+1)} \ f_1(x J_2)$$

$$S'_{inel_4}(b)_{o,f} = \frac{4}{9} \left(\frac{p_1 p_2}{\hbar v} \right)^2 \frac{1}{b^4} \frac{J_2^2 - K_2^2}{J_2(2J_2+1)}$$

$$x \ \frac{K_1^2}{(J_1+1)(J_1+2)} \ f(x J_2)$$

$$S'_{inel_4}(b)_m = \frac{4}{9} \left(\frac{p_1 p_2}{\hbar v} \right)^2 \frac{1}{b^4} \frac{J_2^2 - K_2^2}{J_2(2J_2+1)}$$

$$(-1) \ \frac{2K_1^2}{(J_1+1)^2} \ f_1(x J_2)$$

$$S'_{inel_4}{}^{(b)} = \frac{4}{9} \left(\frac{P_1 P_2}{\hbar v} \right)^2 \frac{1}{b^4} \frac{J_2{}^2 - K_2{}^2}{J_2(2J_2+1)} \frac{K_1{}^2}{J_1(J_1+1)}$$

$$+ \frac{K_1{}^2}{(J_1+1)(J_1+2)} - \frac{2K_1{}^2}{(J+1)^2} f_1(xJ_2)$$

$$S'_{inel} = \frac{4}{9} \left(\frac{P_1 P_2}{\hbar v} \right)^2 \frac{1}{b^4} \left[\frac{k_2}{J_2(J_2+1)} \left\{ \frac{(J_1+1)^2 - K_1{}^2}{(2J_1+1)(J_1+1)} \right. \right.$$

$$f(x(J+1) + \frac{(J_1+2)^2 - K_1{}^2}{(2J_1+3)(J_1+2)} f(x(J_1+2))$$

$$+ \frac{J_1{}^2 - K_1{}^2}{J_1(2J_1+1)} f(xJ_1) + \frac{(J_1+1)^2 - K_1{}^2}{(J_1+1)(2J_1+3)} f_1(x(J_1+1)) \Big\}$$

$$+ \frac{(J_2+1)^2 - K_2{}^2}{(2J_2+1)(J_2+1)} \left\{ \frac{K_1{}^2}{J_1(J_1+1)} + \frac{K_1{}^2}{(J_1+1)(J_1+2)} \right.$$

$$- \frac{2K_1{}^2}{(J_1+1)^2} f_1(x(J_2+1)) + \frac{J_2{}^2 - K_2{}^2}{J_2(2J_2+1)} \frac{K_1{}^2}{J_1(J_1+1)}$$

$$+ \frac{K_1{}^2}{(J_1+1)(J_1+2)} \frac{2K_1{}^2}{(J_1+1)^2} \Big\} f_1(xJ_2)$$

$$\Delta J_1 = 1, \ \Delta J_2 = 1, \quad D = J_1 + J_2 + 2,$$

$$S''_{inel_1}{}^{(b)}{}_{0,1} = \frac{4}{9} \left(\frac{P_1 P_2}{\hbar v} \right)^2 \frac{1}{b^4} (j_1 1 K_i 0 | j_i + 1 K_i)^2$$

$$x(j_2 1 K_2 0 | j_2 + 1 K_2)^2 f_1(x(J_i + J_2 + 2))$$

$$= \frac{4}{9} \left(\frac{P_1 P_2}{\hbar v} \right)^2 \frac{(J_1+1)^2 - K_1{}^2}{(2J_1+1)(J_1+1)}$$

$$x \frac{(J_2+1)^2 - K_2{}^2}{(2J_2+1)(J_2+1)} f_1(x(J_1 + J_2 + 2))$$

$$S''_{inel_2}{}^{(b)}{}_{o,f} = \frac{4}{9} \left(\frac{P_1P_2}{\hbar v} \right)^2 \frac{1}{b^4} \frac{(J_1+2)^2-K_1^2}{(2J_1+3)(J_1+2)}$$

$$\times \frac{(J_2+1)^2-K_2^2}{(2J_2+1)(J_2+1)} f_1(x(J_1+J_2+3))$$

$\Delta J_i = -1. \ \Delta J_2 = -1, \quad D - J_i + J_2$

$$S''_{inel_2}{}^{(b)}{}_{o,i} = \frac{4}{9} \left(\frac{P_1P_2}{hv} \right)^2 \frac{1}{b^4} (j_i 1 K_i 0 | J_i - 1 K_i)^2$$

$$(j_2 1 K_2 0 | j_2 - 1 K_2)^2 \ f_1(x(J_i+J_2))$$

$$= \frac{4}{9} \left(\frac{P_1P_2}{\hbar v} \right)^2 \frac{1}{b^4} \frac{J_1^2-K_1^2}{J_1(2J_1+1)}$$

$$\frac{J_2^2-K_2^2}{J_2(2J_2+1)} f_1(x(J_1+J_2))$$

$$S''_{inel_2}{}^{(b)}{}_{o,i} = \frac{4}{9} \left(\frac{P_1P_2}{\hbar v} \right)^2 \frac{1}{b^4} \frac{(J_1+1)^2-K_1^2}{(J_1+1)(2J_1+3)}$$

$$\frac{J_2^2-K_2^2}{J_2(2J_2+1)} f_1(x(J_1+J_2+1))$$

$$S''_{inel}{}^{(b)} = \frac{4}{9} \left(\frac{P_1P_2}{\hbar v} \right)^2 \frac{1}{b^4} \left[\frac{(J_2+1)^2-K_2^2}{(2J_2+1)(J_2+1)} \right.$$

$$\left\{ \frac{(J_1+1)^2-K_1^2}{(2J_1+1)(J_1+1)} f_1(x(J_1+J_2+2)) \right.$$

$$\left. + \frac{(J_1+2)^2-K_1^2}{(2J_1+3)(J_1+2)} f_1(x(J_1+J_2+3)) \right\}$$

$$+ \frac{J_2^2-K_2^2}{J_2(2J_2+1)} \left\{ \frac{J_1^2-K_1^2}{J_1(2J_1+1)} f_1(x(J_1+J_2)) \right.$$

$$\left. \left. + \frac{(J_1+1)^2-K_1^2}{(J_1+1)(2J_1+3)} f_1(x(J_1+J_2+1)) \right\} \right] .$$

APPENDIX B

THE FORMULATION OF AHFS CRYSTAL POTENTIAL

The crystal potential can be considered as a superposition of atomic potentials. It can be divided into two parts: the Coulomb part and the exchange part. For the Coulomb part

$$V_{cry}^{Coul}(\vec{r}) = \sum_{\vec{R}_\nu} \sum_{i=1}^{2} V_{atomic}^{Coul}[\vec{r} - (\vec{R}_\nu \mp t_i)], \qquad (B.1)$$

where

$$V_{atomic}^{Coul}(\vec{r}) = -\frac{Z}{r} + \frac{4\pi}{r}\int_0^r \rho(r')r'^2 dr' + 4\pi\int_r^\infty (r')r'dr'. \qquad (B.2)$$

$V_{cry}^{Coul}(\vec{r})$ can be expanded in a Fourier series

$$V_{cry}^{Coul}(\vec{r}) = \sum_{K_\nu} V_{cry}^{Coul}(\vec{K}_\nu)\exp(i\vec{K}_\nu\cdot\vec{r}) \qquad (B.3)$$

and $V_{cry}^{Coul}(\vec{K}_\nu)$ is defined as

$$V_{cry}^{Coul}(\vec{K}_\nu) = \frac{1}{N\Omega}\int V_{cry}^{Coul}(\vec{r})\exp(-\vec{K}_\nu\cdot\vec{r})d\tau. \qquad (B.4)$$

Upon substituting (B.3) into (B.4)

$$V_{cry}^{Coul}(\vec{K}_\nu) = \frac{1}{N\Omega}\sum_{\vec{R}_\nu}\sum_{i=1}^{2}\int V_{atomic}^{Coul}[\vec{r}-(\vec{R}_\nu+\vec{t}_i)]\exp(-i\vec{K}_\nu\cdot\vec{r})d\tau$$

$$= \frac{2\cos\vec{K}\cdot\vec{t}}{\Omega}\int V_{atomic}^{Coul}(\vec{r})\exp(-i\vec{K}_\nu\cdot\vec{r})d\tau \qquad (B.5)$$

where $\vec{t} = \vec{t}_2 = -\vec{t}_1$.

Since the choice of the origin of the crystal potential is such that it is invariant under inversion equation (B.5) can be

written as

$$V_{cry}^{Coul}(\vec{K}_{\nu}) = \frac{2\cos\vec{K}_{\nu}\cdot\vec{t}}{\Omega}\int V_{atomic}^{Coul}(\vec{r})\cos\vec{K}_{\nu}\vec{r}d\tau, \tag{B.6}$$

$$\int V_{atomic}^{Coul}(\vec{r})\cos\vec{K}_{\nu}\,\vec{r}d\tau = \int_{0}^{\infty}V_{atomic}^{Coul}(r)r^2 dr$$

$$x\int_{0}^{\pi}\cos(K_{\nu}r\cos\theta)\sin\theta d\theta\int_{0}^{2\pi}d\phi$$

$$= \frac{4\pi}{K_{\nu}}\int_{0}^{\infty}rV_{atomic}^{Coul}(r)\sin(K_{\nu}r)dr\ .$$

Therefore

$$V_{cry}^{Coul}(\vec{K}_{\nu}) = \frac{8\pi\cos\vec{K}\cdot\vec{t}}{K_{\nu}}\int_{0}^{\infty}rV_{atomic}^{Coul}(r)\sin(K_{\nu}r)dr\ . \tag{B.7}$$

Substituting (B.2) into (B.7) and effecting the integration

yields

$$V_{cry}^{Coul}(\vec{K}_{\nu}) = \frac{-8\pi\cos\vec{K}_{\nu}\cdot\vec{t}}{K_{\nu}^{2}\Omega}\left\{Z-4\pi\int_{0}^{\infty}r^2\rho(r)\frac{\sin K_{\nu}r}{K_{\nu}r}\ dr\ . \tag{B.8}$$

For the exchange part, we use the standard Slater exchange

approximation

$$V_{atomic}^{exch}(r) = -3[\frac{3}{8\pi}\rho(r)]^{\frac{1}{3}}\ . \tag{B.9}$$

$$V_{cry}^{exch}(\vec{r}) = \sum_{\vec{R}}\sum_{i=1}^{2}V_{atomic}^{exch}[\vec{r}-(\vec{R}_{\nu}+\vec{t}_{i})]$$

$$V_{cry}^{exch}(\vec{K}_{\nu}) = \frac{1}{N\Omega}\int V_{cry}^{exch}(\vec{r})\exp(-i\vec{K}_{\nu}\cdot\vec{r})d\tau$$

$$= \frac{8\pi\cos\vec{K}_{\nu}\cdot\vec{t}}{k}(\frac{3}{8\pi})^{\frac{1}{3}}\int_{0}^{\infty}r[\rho(r)]^{\frac{1}{3}}$$

$$x\sin(K_{\nu}r)dr\ . \tag{B.10}$$

The crystal potential is a sum of the Coulomb and exchange terms,

$$V_{cry}(\vec{r}) = V_{cry}^{exch}(\vec{r}) + V_{cry}^{Coul}(\vec{r})$$

$$= \sum_{K_\nu} V_{cry}(\vec{K_\nu}) \cos \vec{K_\nu} \cdot \vec{r} . \tag{B.11}$$

and we obtain

$$V_{cry}(\vec{K_\nu}) = V_{cry}^{Coul}(\vec{K_\nu}) + V_{cry}^{exch}(\vec{K_\nu})$$

$$= -\frac{8\pi}{K_\nu^2 \Omega} \cos \vec{K_\nu} \cdot \vec{t} \left\{ Z - \frac{1}{K_\nu} \int_0^\infty Q(r) \sin K_\nu r \, dr \right.$$

$$\left. + K_\nu \int_0^\infty E(r) \sin K_\nu r \, dr \right. , \tag{B.12}$$

where

$$Q(r) = 4\pi r \rho(r),$$

$$E(r) = \frac{3}{2} [3\rho(r)/\pi]^{\frac{1}{3}} .$$

APPENDIX C

THE EWALD-TYPE POTENTIAL EXPANSION

In chapter IX, we divide the crystal potential into two parts,

$$V(\vec{r}) = V_1(\vec{r}) + [V(\vec{r}) - V_1(\vec{r})] ,$$

$$V_1(\vec{r}) = \sum_{\mu} \mathcal{V}(\vec{r} - \vec{R}_{\mu}) ,$$

where the requirement for $\mathcal{V}(r)$ is such that it behaves like Z/r near the origin. The part $V_2(\vec{r}) = V(\vec{r}) - V_1(\vec{r})$ is in effect a "cut-off" potential with the singularity cut off. Therefore $V_2(\vec{r})$ is a relatively smooth function of r and consequently requires less number of Fourier coefficients to represent it. As shown in the calculation of lithum band structure by Gaussian basis functions[37] we can approximate

$$< G(\alpha_1, \vec{r} - \vec{A}) | V_1(\vec{r}) | G(\alpha_2, \vec{r} - \vec{B}) >$$

$$\approx < G(\alpha_1, \vec{r} - \vec{A}) | \mathcal{V}(\vec{r} - \vec{A}) | G(\alpha_2, \vec{r} - \vec{A}) > .$$

In the process of subtracting $V_1(\vec{r})$ and form $V_2(\vec{r})$, we have

$$V(\vec{K}_{\mu}) = \frac{1}{N\Omega} \int V_1(\vec{r}) \exp(-i\vec{K}_{\mu} \cdot \vec{r}) d\tau$$

$$= \frac{8\pi \cos \vec{K}_{\mu} \cdot \vec{t}}{K_{\mu} \Omega} \int_0^{\infty} r \mathcal{V}(r) \sin K_{\mu} r \, dr , \qquad (C.1)$$

assuming that $\mathcal{V}(r)$ can be written as

$$\mathcal{V}(r) = \frac{1}{r}(Z + a_1 r + a_2 r^2 + \ldots \ldots) \exp(-br^2)$$

$$= \frac{1}{r}(Z + \sum_{i=1}^{n} a_i r^i) \exp(-br^2)$$

79

where b is chosen with an appropriate magnitude such that $\mathcal{V}(r)$ remains well localized.

$$V_1(\vec{K}_\nu) = \frac{8\pi\cos\vec{K}_\nu\cdot\vec{t}}{K_\nu\,\Omega}\left\{Z\int_0^\infty \exp(-br^2)\sin K_\nu r\,dr\right.$$

$$\left. + \sum_{i=1}^n a_i\int_0^\infty r^i\exp(-br^2)\sin K_\nu r\,dr\right. \quad . \tag{C.2}$$

The integral of the type $\int_0^\infty x^{2\nu-2}\,e^{-\alpha x^2}\sin(yx)dx$ is evaluated by using Hypergeometric function and Gamma function[52] such that

$$\int_0^\infty x^{2\nu-2}\exp(-\alpha x^2)\sin(yx)dx$$

$$= \tfrac{1}{2}\alpha^{-\nu}\Gamma(\nu)y\;F_1(\nu;\tfrac{3}{2};-\tfrac{1}{4}y^2/\alpha) \quad . \tag{C.3}$$

In the case of diamond, we use

$$\mathcal{V}(r) = -(\tfrac{Z}{r})(1+\mu r^2)\exp(-\mu r^2)$$

with $\mu = 2.5$.

In the case of MgO, we obtain the "cut-off" potentials for both magnesium and oxygen and then form the symmetric and antisymmetric parts of the crystal potential. In MgO, instead of fixing the values of b and a_i's, we let the high Fourier coefficients be the $V_1(\vec{K}_\nu)$ and using

$$V(r) = \frac{1}{r}\left\{\alpha\exp(-\beta_1 r^2) - (Z+\alpha)\exp(-\beta_2 r^2)\right\} \quad . \tag{C.4}$$

The α and β's are not pre-determined but were fitted by a least-square curve-fitting such that $V_1(\vec{K}_\nu)$ will be the same as the tail part of $V(\vec{K}_\nu)$. The values of α, β_1, and β_2 for magnesium are

$$\alpha = -14.7853, \quad \beta_1 = 19.3866, \quad \beta_2 = 60.3715,$$

and for oxygen are

$$\alpha = -9.94075, \quad \beta_1 = 16.8809, \quad \beta_2 = 66.8269 \quad .$$

We list in table XV and table XVI the comparison of $V_2(\vec{K}_\nu)$ and $V(\vec{K}_\nu)$ which we call V_{K_ν} and V_{2K_ν}.

To evaluate the integral

$$\langle G^s(\alpha_1, \vec{r}_A) | V(\vec{r}_A) | G^s(\alpha_2, \vec{r}_B) \rangle \quad \text{for } \alpha_1 \gg \alpha_2$$

we use the scheme of expanding $\exp(-\alpha_2 r_B^2)$ about the point A in Taylor series and then integrate the series until it reaches convergence. For the $-Z/r_A$ term, the integral has the form

$$I = -\int \exp(-\alpha_1 r_A^2)(Z/r_A)\exp(-\alpha_2 r_B^2)d\tau \ .$$

Since

$$\vec{r}_B = \vec{r}_A - \vec{AB} \ ,$$

so

$$r_B^2 = r_A^2 + \overline{AB}^2 - 2\vec{r}_A \cdot \vec{AB}$$

$$= r_A^2 + \overline{AB}^2 - 2r_A \overline{AB}\cos\theta \ ,$$

where θ is the angle between $\vec{r}_A$ and $\vec{r}_B$. We can therefore write

$$\exp(-\alpha_2 r_B^2) = \exp(-\alpha_2(r_A^2 + \overline{AB}^2)) \exp(2\ _2 r_A \overline{AB}\cos\theta)$$

and expand the second exponent as

$$\exp(2\alpha_2 r_A \overline{AB}\cos\theta) \simeq 1 + \sum_n \frac{(2\alpha_2 r_A \overline{AB}\cos)^n}{n!} \ .$$

The integral now becomes

$$I = -Z\exp(-\alpha_2 \overline{AB}^2) \int r_A \exp(-(\alpha_1 + \alpha_2)r_A^2)$$

$$\times \sum_{n=0}^{\infty} \frac{(2\alpha_2 r_A \overline{AB}\cos\theta)^n}{n!} \sin\theta d\theta d\phi dr$$

$$= -2\pi Z\exp(-\alpha_2 AB^2) \sum_{n=0}^{\infty} (\frac{2\alpha_2 \overline{AB}}{n!})^n$$

$$\times [\int_0^{\infty} r_A^{n+1} \exp(-(\alpha_1 + \alpha_2)r_A^2)dr]$$

$$\times [\int_0^{\pi} \cos^n\theta \sin\theta d\theta]$$

$$= -4\pi Z\exp(-\alpha_2 \overline{AB}^2) \sum_{n=0}^{\infty} \frac{(2\alpha_2 \overline{AB})^{2n}}{(2n+1)!} \int_0^{\infty} r_A^{2n+1} \exp(-(\alpha_1 + \alpha_2)r_A^2)dr_A \ .$$

The radial part of the integral is of the form

$$\int_0^\infty r^{2n+1} \exp(-\lambda r^2) dr = \frac{n!}{2\lambda^{n+1}} \quad .$$

If the purpose is to evaluate $(-Z/r)^{\nu} r^2$ then the only modification will be

$$\int_0^\infty r^{2(n+1)+1} \exp(-\lambda r^2) dr = \frac{(n+1)!}{2\lambda^{n+2}} \quad .$$

Therefore, the result for $-Z/r$ can also be used for $(-Z/r)^{\nu} r^2$ provided that we multiply the result of the former by a factor of $\nu(n+1)/\lambda$. The integral I is evaluated as

The integral I is evaluated as

$$I = -2 \; Z\exp(-\alpha_2 \overline{AB}^2) \sum_{n=0}^{\infty} \frac{(2\alpha_2 \overline{AB})^{2n}}{(2n+1)!} \; \frac{n!}{(\alpha_1 + \alpha_2)^{n+1}}$$

The convergence of the summation is dictated by the ratio of the nth term with respect to the sum of the (n-1) terms. If the ratio is less than 10^{-6}, we stop the summation.

The s-p, and p-p integral again could be obtained by partial differentiation with respect to B_x, B_y or B_z:

$$\left\langle G^s(\alpha_1, \vec{r}_A) \; \middle| \; -\frac{Z}{r_A} \middle| G^{P_x}(\alpha_2, \vec{r}_B) \right\rangle$$

$$= \frac{1}{2\alpha_2} \frac{\partial}{\partial B_x} \left\langle G^s(\alpha_1, \vec{r}_A) \; \middle| \; -\frac{Z}{r_A} \middle| G^s(\alpha_2, \vec{r}_B) \right\rangle$$

$$= 2\pi Z\exp(-\alpha_2 \overline{AB}^2) \vec{AB} \; [\sum_{n=0}^{\infty} \frac{(2\alpha_2 \overline{AB})^{2n}}{(2n+1)!} \; \frac{n!}{(\alpha_1 + \alpha_2)^{n+1}}$$

$$- 4\alpha_2 \sum_{n=1}^{\infty} \frac{n(2\alpha_2 \overline{AB})^{2n-2}}{(2n+1)!} \; \frac{n!}{(\alpha_1 + \alpha_2)^{n+1}}] \; .$$

$$\langle G^{Px}(\alpha_1, \vec{r}_A) \mid -\frac{Z}{r_A} \mid G^s(\alpha_2, \vec{r}_B) \rangle$$

$$= -\frac{2\pi Z}{\alpha_2} \exp(-\alpha_2 \overline{AB}^2) \overline{AB}_x \sum_{n=1}^{\infty} \frac{n! (2\alpha_2)^{2n}}{(2n+1)! (\alpha_1+\alpha_2)^{n+1}} n(\overline{AB}^2)^{n-1}$$

$$\langle G^{Px}(\alpha_1, \vec{r}_A) \mid -\frac{Z}{r_A} \mid G^{Py}(\alpha_2, \vec{r}_B) \rangle$$

$$= -\frac{\pi Z}{\alpha_2^2} \exp(-\alpha_2 \overline{AB}^2) \overline{AB}_x \overline{AB}_y \sum_{n=1}^{\infty} \frac{(2\alpha_2)^{2n} n!}{(2n+1)! (\alpha_1+\alpha_2)^{n+1}}$$

$$\times \left\{ n(n-1)(\overline{AB}^2)^{n-2} - 2\alpha_2 n(\overline{AB}^2)^{n-1} \right\}. \qquad [53]$$

TABLE XV

COMPARISON OF V_{K_μ} AND V_{2K_μ} FOR DIAMOND

K_x	K_y	K_z	V_{K_μ}	V_{2K_μ}
0	0	0	-1.435	-0.64276
2	2	0	-0.20803	0.19417
4	0	0	-0.11484	0.10115
4	2	2	-0.080940	0.045115
5	1	1	-0.073118	0.032615
5	3	1	-0.58377	0.012904
5	3	3	-0.048701	0.0019987
5	5	1	-0.041788	0.0011086
6	4	2	-0.038372	0.00023358
7	3	1	-0.036572	-0.000049802

TABLE XVI

COMPARISON OF V_{K_y} AND V_{2K_y} FOR Mg and O

K_x	K_y	K_z	$V_{K_y}(0)$	$V_{2K_y}(0)$	$V_{K_y}(Mg)$	$V_{2K_y}(Mg)$
9	5	1	-0.1115×10^{-1}	0.2426×10^{-2}	-0.1607×10^{-1}	0.5833×10^{-2}
23	11	7	-0.1817×10^{-2}	0.1999×10^{-3}	-0.2717×10^{-2}	0.2440×10^{-3}
30	8	2	-0.1319×10^{-2}	0.5143×10^{-4}	-0.1968×10^{-2}	0.5562×10^{-4}
31	11	1	-0.1182×10^{-2}	0.2940×10^{-4}	-0.1761×10^{-2}	0.2923×10^{-4}
30	16	14	-0.9487×10^{-3}	0.8585×10^{-5}	-0.1412×10^{-2}	0.5213×10^{-5}
39	7	7	-0.7753×10^{-3}	0.3368×10^{-5}	-0.1181×10^{-2}	0.4302×10^{-7}

APPENDIX D

KINETIC AND POTENTIAL INTEGRALS

The integrals of kinetic and potential energies are as follows:

$$\langle G^s(\alpha_1, \vec{r}-\vec{A}) \mid -\tfrac{1}{2}\nabla^2 \mid G^s(\alpha_2, \vec{r}-\vec{B}) \rangle = \lambda\Delta\zeta(3 - 2\lambda\overline{AB}^2),$$

$$\langle G^{px}(\alpha_1, \vec{r}-\vec{A}) \mid -\tfrac{1}{2}\nabla^2 \mid G^s(\alpha_2, \vec{r}-\vec{B}) \rangle = \lambda^2\Delta\zeta\overline{AB}_x(5-2\lambda\overline{AB}^2)/\alpha_1,$$

$$\langle G^{px}(\alpha_1, \vec{r}-\vec{A}) \mid -\tfrac{1}{2}\nabla^2 \mid G^{px}(\alpha_2, \vec{r}-\vec{B}) \rangle = \lambda^2\Delta\zeta(\tfrac{5}{2} - 7\lambda\overline{AB}_x^2 - \lambda\overline{AB}^2 + 2\lambda^2\overline{AB}^2\overline{AB}_x^2)/\alpha_1\alpha_2,$$

$$\langle G^{px}(\alpha_1, \vec{r}-\vec{A}) \mid -\tfrac{1}{2}\nabla^2 \mid G^{py}(\alpha_2, \vec{r}-\vec{B}) \rangle = \lambda^3\Delta\zeta\overline{AB}_x\overline{AB}_y(2\lambda\overline{AB}^2 - 7)/\alpha_1\alpha_2,$$

$$\langle G^s(\alpha_1, \vec{r}-\vec{A}) \mid \cos(\vec{K}_\nu\cdot\vec{r}_c) \mid G^s(\alpha_2, \vec{r}-\vec{B}) \rangle = \Delta\delta\zeta\cos(\vec{K}_\nu\cdot\vec{r}_{CD}),$$

$$\langle G^{px}(\alpha_1, \vec{r}-\vec{A}) \mid \cos(\vec{K}_\nu\cdot\vec{r}_c) \mid G^s(\alpha_2, \vec{r}-\vec{B}) \rangle =$$

$$= \Delta\delta\zeta[(\lambda\overline{AB}_x/\alpha_1)\cos(\vec{K}_\nu\cdot\vec{r}_{CD})$$

$$- (\vec{K}_\nu)_x \sin(\vec{K}_\nu\cdot\vec{r}_{CD})/2(\alpha_1+\alpha_2)],$$

$$\langle G^{px}(\alpha_1, \vec{r}-\vec{A}) \mid \cos(\vec{K}_\nu\cdot\vec{r}_c) \mid G^{px}(\alpha_2, \vec{r}-\vec{B}) \rangle = \Delta\delta\zeta\{(\lambda/\alpha_1\alpha_2)[\tfrac{1}{2} - \lambda\overline{AB}_x^2$$

$$- (\lambda/4\alpha_1\alpha_2)(\vec{K}_\nu)_x^2]\cos(\vec{K}_\nu\cdot\vec{r}_{CD})$$

$$+ (\lambda/2\alpha_1\alpha_2)\overline{AB}_x(\vec{K}_\nu)_x(2u-1)\sin(\vec{K}_\nu\cdot\vec{r}_{CD})\},$$

$$\langle G^{px}(\alpha_1, \vec{r}-\vec{A}) \mid \cos(\vec{K}_\nu\cdot\vec{r}_c) \mid G^{py}(\alpha_2, \vec{r}-\vec{B}) \rangle$$

$$= (\lambda/\alpha_1\alpha_2)\Delta\delta\zeta\{\tfrac{1}{2}[u(\vec{K}_\nu)_x\overline{AB}_y$$

$$- (1-u)(\vec{K}_\nu)_y\overline{AB}_x]\sin(\vec{K}_\nu\cdot\vec{r}_{CD})$$

$$- \lambda[\overline{AB}_x\overline{AB}_y + (\vec{K}_\nu)_x(\vec{K}_\nu)_y/4\alpha_1\alpha_2]\cos(\vec{K}_\nu\cdot\vec{r}_{CD})\},$$

where

$$\lambda = \alpha_1 \alpha_2 / (\alpha_1 + \alpha_2), \quad \Delta = [\pi / (\alpha_1 + \alpha_2)]^{3/2}, \quad \Im = \exp(-\lambda \overline{AB}^2),$$

$$\delta = \exp[-K_\nu^2 / 4(\alpha_1 + \alpha_2)], \qquad u = \alpha_1 / (\alpha_1 + \alpha_2),$$

and $\overline{AB}_x$ refers to the x component of the line joining the points A and B.

LIST OF REFERENCES

1. A. A. Michelson, Astro. Phys. J. 2, 251 (1895).

2. H. A. Lorentz, Proc. Acad. Sci. Amst. 8, 591 (1906).

3. V. Weisskopf, Z. Physik 75, 287 (1932).

4. A. Jablonski, Phys. Rev. 68, 78 (1945).

5. H. M. Foley, Phys. Rev. 69, 616 (1946).

6. E. Lindholm, Ark. Mat. Astron. Fys. A32, 17 (1945).

7. H. Margenau and W. S. Watson, Rev. Mod. Phys. 8, 22 (1936).

8. W. V. Smith, Ann. N. Y. Acad. Sci. 55, 891 (1952).

9. W. V. Smith, J. Chem. Phys. 25, 510 (1955).

10. G. Birnbaum, Advan. Chem. Phys. 12, 487 (1967).

11. P. W. Anderson, Phys. Rev. 76, 647 (1949).

12. C. J. Tsao and B. Curnutte, J. Quant. Spectry. Radiative Transfer 2, 41 (1962).

13. J. Cooper, Rev. Mod. Phys. 39, 167 (1967).

14. C. O. Trindale and K. H. Illinger, J. Chem. Phys. 46, 3429 (1967).

15. J. S. Murphy and J. E. Boggs, J. Chem. Phys. 47, 691 (1967).

16. J. S. Murphy and J. E. Boggs, J. Chem. Phys. 47, 4152 (1967).

17. H. Margenau and S. Bloom, Phys. Rev. 90, 791 (1953).

18. C. H Townes and A. L. Schawlow, Microwave Spectroscopy (McGraw-Hill Book Co., Inc., New York, 1955).

19. G. Birnbaum, J. Chem. Phys. 46, 2455 (1967).

20. E. U. Condon and G. H. Shortly, *The Theory of Atomic Spectra* (Cambridge Univ. Press, London, 1963).

21. M. E. Rose, *Elementary Theory of Angular Momentum* (J. Wiley and Sons, Inc., New York, 1957).

22. I. S. Sokolnikoff and E. S. Sokolnikoff, *Higher Mathematics for Engineers and Physicists* (McGraw-Hill Book Co., Inc., New York, 1941).

23. L. D Landau and E. M. Lifshitz, *Statistical Physics* (Pergamon Press, London, 1958).

24. P. Kisliuk and C. H. Townes, *Molecular Microwave Spectra Tables*, Natl. Bur. Std. (U.S.) Circ. No. 518 (1952).

25. J. A. Roberts, T. K. Tung, and C. C. Lin, J. Chem. Phys. $\underline{48}$ 4046 (1968).

26. R. L. Legan, J. A. Roberts, E. A. Rinehart, and C. C. Lin, J. Chem. Phys. $\underline{43}$, 4337 (1965).

27. See, for example, *Methods in Computational Physics*, edited by B. Alder, S. Fernbach, and M. Rotenberg, vol. 8 (Academic Press Inc., New York, 1968; J. Callaway, *Energy Band Theory* (Academic Press Inc., New York, 1964); J. C. Slater, *Quantum Theory of Molecules and Solids* Vol. 2 (McGraw-Hill Inc., New York, 1965).

28. F. Herman, R. L. Kortum, C. D. Kuglin, and R. A. Short, J. Phys. Soc. (Japan) $\underline{21}$, Supplement 7 (1966).

29. See, for example, C. Y. Fong, W. Saslow, and M. L. Cohen, Phys. Rev. $\underline{168}$, 992 (1968).

30. F. Bloch, Z. Physik $\underline{52}$, 555 (1928).

31. J. C. Slater and G. F. Koster, Phys. Rev. $\underline{94}$, 1498 (1954).

32. E. E. Lafon and C. C. Lin, Phys. Rev. $\underline{152}$, 529 (1966).

33. I. Shavitt in *Methods in Computational Physics*, edited by B. Alder, S. Fernbach, and M. Rotenberg (Academic Press Inc., New York, 1963).

34. E. E Lafon and C. C. Lin, Private communication.

35. S. F. Boys, Proc. Roy. Soc. $\underline{A200}$, 452 (1950).

36. See, for example, E. Clementi, J. Chem. Phys. <u>46</u>, 3851 (1967); Chem. Rev. <u>68</u>, 341 (1968); S. Huzinaga, J. Chem. Phys. <u>42</u>, 1293 (1965); S. Huzinaga and Y. Sakai, J. Chem. Phys. <u>50</u>, 1371 (1969); S. Salezard and A. Velliard Theoret. Chim. Acta. (Berl.) <u>11</u>, 441 (1968); A. Velliard, Theoret. Chim. Act. (Berl.) <u>12</u>, 405 (1968).

37. R. C. Chaney, T. K. Tung, C. C. Lin and E. E. Lafon, J. Chem. Phys., <u>52</u>, 361 (1970).

38. D. R. Hartree, <u>The Calculation of Atomic Structures</u> (John Wiley and Son, Inc., New York 1957).

39. T. O. Woodruff, Solid State Phys. <u>4</u>, 367 (1957).

40. W. Kohn and L. J. Sham, Phys. Rev. <u>140</u>, A1133 (1965), I. Goroff and L. Kleinman, Phys. Rev. <u>164</u>, 1100 (1967).

41. E. E. Lafon, Private communication.

42. A. Jucys, Proc. Roy. Soc. (London) <u>A175</u>, 59 (1939).

43. F. Bassani and M. Yoshimini, Phys. Rev. <u>130</u>, 20 (1963).

44. L. P. Bouckart, R. Smoluchowski, and E. P. Wigner, Phys. Rev. <u>50</u>, 58 (1936).

45. S Huzinaga, J. Chem. Phys. <u>42</u>, 1293 (1965).

46. C. Kittel, <u>Quantum Theory of Solids</u> (John Wiley and Son, Inc., New York, 1963).

47. E. Clementi, <u>Tables of Atomic Functions</u>, Supplement to IBM J. of Res. Develop. <u>9</u>, 1 (1965).

48. R. F. Stewart, J. Chem. Phys. <u>50</u>, 2485 (1969).

49. H. Hosoya, J. Chem. Phys. <u>48</u>, 1380 (1968).

50. The program was written by E. E. Lafon.

51. A. Trefftz and L. Bierman, Z. Astrophys. <u>26</u>, 213 (1949).

52. <u>Tables of Integral Transformations</u>, edited by A. Erdelyi (McGraw-Hill Book Co., Inc., New York 1954).

53. The program was written by R. C Chaney.

54. R. A. Roberts, D. M. Roessler, and W. C. Walker, Phys. Rev. Letters <u>17</u>, 302 (1966).